SAND2010-6293P

Luminescent Metal-Organic Frameworks

John J. Perry IV[§], Christina A. Bauer[†], and Mark D. Allendorf[§]*

[§] Dept. of Energy Nanomaterials, Sandia National Laboratories,

Livermore, CA 94550-0969

[†] Dept. of Chemistry and Biochemistry, University of California

Los Angeles, CA 90095-1569

1 Introduction

Luminescence is an oft-reported property of metal-organic frameworks (MOF), in large part because these structures typically contain aromatic or conjugated linker groups that readily fluoresce, or incorporate luminescent lanthanide ions. Because the moieties are largely immobilized by the crystal structure, lifetimes and quantum efficiencies may be higher than those exhibited by the isolated luminophore in solution. MOFs are not completely rigid, however; their well-known structural flexibility can lead to dramatic changes in local coordination environment and corresponding variations in emissive properties. The nanoporosity of these structures also creates new opportunities to impart light-emitting properties that are not available to traditional inorganic complexes. In particular, infiltrated guest molecules that are themselves emitters or sensitizers can be immobilized in close proximity to luminescent centers. This can influence the emission properties of the neat MOF in the form of wavelength shifts, intensity changes, or new emission resulting from excimer or exciplex formation. Since fluorescence spectrometers are readily available, many investigators report the excitation and emission spectra of newly synthesized MOF structures. As a result, more than 300 reports of luminescent MOFs are now in the literature. Relatively few studies delve into the underlying spectroscopy or use luminescence as a tool for probing electronic structure and energy transfer. Nevertheless, it is apparent that luminescence holds considerable potential to serve not only as a diagnostic tool for probing fundamental aspects of MOF behavior and structure, but also show potential for a variety of applications. As might be expected, chemical sensing is a logical possibility, but as will be seen later in this chapter, the potential extends well beyond this to include radiation detection, non-linear optical effects, and solid-state lighting.

The purpose of this chapter is first to introduce the reader to the basic concepts of luminescence relevant to much of the current MOF literature. We then discuss luminescence associated with individual components of MOFs, each of which displays characteristic features. Examples from recent literature are provided that illustrate the multidimensional character of MOF luminescence. However, a comprehensive review is not presented, as was recently done [1]. As will be seen, a detailed understanding of luminescence phenomena in MOFs is beginning to emerge. Although still in its early stages, the results demonstrate that the unique characteristics of these supramolecular materials provide a platform for understanding light emission with both unparalleled synthetic flexibility and a highly ordered, inherently quantifiable, structure. From a practical point of view, it is also becoming clear that

luminescence spectroscopy is a superb tool for assessing the structural integrity and purity of MOFs, with sensitivity far exceeding that of powder X-ray diffraction. The chapter concludes with an overview of recent developments concerning applications of luminescent MOFs.

2 Luminescence Theory

In general, luminescence is the result of radiative decay (*i.e.* emission of light) by electronically excited molecules following the absorption of energy. The absorbed energy can originate from a variety of sources, which leads to different sub-classifications of luminescence. When the energy is absorbed from electromagnetic radiation in the form of photons (light), the subsequent emission of light is defined as *photoluminescence*. The non-thermal production of light by a chemical reaction is termed *chemiluminescence* [2-4], with the special case involving living organisms being referred to as *bioluminescence* [5-7]. In some cases, the presence of an electric field can cause electron-hole recombination in a material, producing *electroluminescence* [8-9]. If the energy absorbed by the molecules is due to the material being bombarded with high energy ionizing radiation (> 10 eV), the emission of light is referred to as *radioluminescence* while a beam of high energy electrons imparted upon a material may lead to *cathodoluminescence*. Additionally, mechanical forces [10-12] acting on a material may also lead to the emission of light in the form of *triboluminescence* (mechanical stress, scratching, or fracture) or *piezoluminescence* (pressure). While there appear to be several methods to electronically excite a molecule or group of molecules in a MOF to yield emission of light, to date only a few have been investigated, the most prevalent of which has been photoluminescence (PL).

2.1 Photoluminescence

While many excellent texts are available concerning the theory of luminescence in general [13-15] and photoluminescence [16-17] in particular, a general, albeit simplified overview of the concepts is warranted. For the sake of simplicity in describing the photophysical processes in question, let us consider only the organic molecule, which acts as a linker or strut in the formation of the MOF. Before a molecule is excited by the absorption of light, the molecule resides in its lowest electronic energy level or ground state. Typically, an organic molecule has a singlet ground state (S_0), but in rare cases a triplet ground state (T_0) is possible. Higher energy electronic states exist (S_n or T_n ; $n \geq 1$), and it is these elevated states to which an electron is promoted upon the absorption of energy. Additionally, each electronic state is associated with several vibrational energy levels and together the electronic and vibrational levels constitute a vibronic state ($S_{n,\nu}$: $\nu = 0,1,2,3,\ldots$). A Jablonski diagram (Fig. 1) is a simplified graphical representation of the vibronic states for a given molecule wherein higher energy levels are stacked vertically over lower ones. Jablonski diagrams are useful for depicting the various photophysical processes involved in the absorption and eventual loss of excess energy by the molecule, but do not account for geometric distortions. The vertical nature of the transitions is reflective of the fact that absorption occurs in a time frame too short for significant relocation of nuclei (Franck–Condon principle) and thus rearrangement of electronic energy states is negligible.

Figure 1.

In the ground state, nearly all of the molecules exist in the lowest totally symmetric (a_1) vibrational level ($S_{0,0}$) at room temperature, and so it is from this vibronic state that absorption of energy leads to excitation to elevated energy levels. In order to sufficiently energize a molecule and promote it to a higher electronic state the use of ultraviolet (UV) or visible light is required. Light of lower energy (and longer wavelength) such as infrared (IR) is typically not energetic enough to cause promotion to higher electronic states, but can be useful for the excitation of higher vibrational levels of the ground electronic state. Upon excitation, the molecule begins to rapidly lose excess vibrational and electronic energy to the surrounding medium (when in a condensed phase) in a non-radiative thermal deactivation process. In the first phase, the molecule loses excess vibrational energy through vibrational relaxation (*VR*), in which the molecule undergoes a radiationless transition from a higher vibrational level to a lower one within the same electronic state. This is followed by a radiationless transition between electronic states of the same multiplicity called internal conversion (*IC*) and possibly further *VR* within the new electronic state. Taken together *VR* and *IC* constitute thermal deactivation of the molecule carrying it to the lowest vibrational level of the lowest excited state in short order (10^{-13} – 10^{-12} s). From the $S_{1,0}$ excited state, the molecule can undergo deactivation *via* one of three first-order processes. For many molecules it is possible to become deactivated by non-radiative internal conversion (rate constant k_{ic}). However, for some molecules containing relatively large gaps in energy between the lowest excited and ground states this process is unfavorable, and the majority of these surrender their excess energy *via* the spin-allowed emission of light known as fluorescence (*F*, k_f). The third possibility is the formally spin-forbidden intersystem crossing (*ISC*, k_{isc}) to the lowest excited triplet state T_1. The excited triplet state must also undergo deactivation and can do so through either spin-forbidden radiative emission known as phosphorescence (*P*, k_p) or though non-radiative spin-forbidden intersystem crossing ($k_{isc'}$).

As there are several competing pathways for the deactivation of the lowest excited singlet state, the number of molecules that fluoresce is but a fraction of the total population of excited molecules. This ratio between the number of molecules which fluoresce and the total excited population is the fluorescence efficiency or *quantum yield of fluorescence* (Φ_f). The quantum yield is a value between 0 (no fluorescence) and 1 (all excited molecules fluoresce) and is related to the first-order rate constants for the deactivation pathways (eq. 1). Similarly, the ratio of the number of molecules to undergo phosphorescence to the number of molecules to be deactivated in any of the other processes is given by a related equation (eq. 2).

$$\Phi_f = \frac{k_f}{k_{ic} + k_f + k_{isc}} \qquad \text{(eq. 1)}$$

$$\Phi_p = \frac{k_p k_{isc}}{(k_{isc'} + k_p)(k_{ic} + k_f + k_{isc})} \qquad \text{(eq. 2)}$$

Another useful property of photoluminescence, especially in the comparison of fluorescence and phosphorescence, is the concept of the lifetime (τ) of a given excited state. The *lifetime* is defined as the average time the molecule exists in the excited state before the excited population is reduced by a factor of *e* (exponential decay). The lifetime of an excited state is therefore the inverse of the summation of the rate constants for the potential decay pathways deactivating that state and is given by the following equations (eq. 3 and eq. 4).

$$\tau(S_1) = \frac{1}{k_{ic} + k_f + k_{isc}} \qquad \text{(eq. 3)}$$

$$\tau(T_1) = \frac{1}{k_{isc'} + k_p} \quad \text{(eq. 4)}$$

The *natural* lifetime (τ_n) is the intrinsic lifetime of the luminophore in the absence of non-radiative decay and can be calculated from the ratio of τ to Φ. As the processes involved in deactivation of S_1 through the T_1 excited state are all spin-forbidden, the lifetimes are typically much longer for phosphorescence (10^{-4} – 10^{0} s) than that observed for fluorescence (10^{-11} – 10^{-7} s).

2.2 Fluorescence Quenching

While many types of molecule are capable of absorbing energy to become electronically excited, relatively few exhibit the phenomenon of luminescence. This is due in part to *quenching*. Essentially, any process capable of diminishing the intensity of fluorescence or phosphorescence can be considered a quenching mechanism [18], including the rapid non-radiative de-excitation of $S_1 \rightarrow S_0$ *via* internal conversion. External molecules called quenchers are also capable of de-exciting a molecule; this will either diminish or completely eliminate the ability of the excited molecule to luminesce. Quenching in MOFs is important from an applications aspect as it can be both detrimental, leading to a reduction in the desired property (luminescence), and beneficial in cases where the quenching of a known luminescence signal is used as a sensor mechanism for detecting the presence of the quencher moiety. Luminescence quenching is observed in one of two forms, *Dynamic* or *Static*. Dynamic quenching is characterized by the collision of a quencher moiety (acceptor) with an excited-state luminophore (donor), resulting in de-excitation of the donor and concomitant excitation of the acceptor. The newly excited acceptor may or may not be luminescent in its own right, but any resulting emission will always be of lower intensity than what would be observed from the donor. In dynamic quenching, the quencher and potential luminophore must come into contact during the lifetime of the luminophore excited state, and is therefore a time-dependent process. Additionally, dynamic quenching is dependent on the concentration [Q] and diffusion of the quencher molecule and obeys the Stern–Volmer equation (eq. 5). In static quenching, interaction between a potential luminophore and a quencher molecule takes place in the ground state, leading to the formation of a non-luminescent complex. Here the efficiency of quenching is governed by the rate of complex formation (k_c) and [Q] (eq. 6).

$$\frac{\Phi}{\Phi_o} = \frac{1}{1 + k_q \tau_o [Q]} \quad \text{(eq. 5)}$$

$$\frac{\Phi}{\Phi_o} = \frac{1}{1 + k_c [Q]} \quad \text{(eq. 6)}$$

2.3 Energy Transfer

Another important process that can affect the luminescence of MOFs is energy transfer (ET). It may be possible, during the lifetime of the excited state, to transfer the excitation energy from an excited molecule (donor) to another molecule in the ground state (acceptor). This is essentially another method of quenching the donor molecule as it will become de-excited and no longer luminescent. The acceptor absorbs the energy and is excited, which may lead to luminescence (albeit at a lower intensity), or it may deactivate *via* a non-radiative pathway so that as a system the luminescence will be lost. There are two mechanisms for ET distinguished by the nature of

the donor-acceptor interaction. In *Förster resonance energy transfer* (FRET; Förster-type; dipole mechanism; coulombic mechanism) the donor and acceptor molecules are not in contact and can be separated by as much as 10 nm [13,18-19]. For FRET to occur at least some spectral overlap between the emission of the donor and the excitation of the acceptor must exist and the rate of energy transfer (probability) is dependent on both the amount of overlap as well as the distance between the two molecules, with the rate decreasing in relation to $(1/r)^6$. In *excitation energy transfer* (Dexter-type; exchange mechanism) the orbitals of the donor and acceptor molecules must be in direct contact. Dexter-type ET is sometimes considered as a double electron transfer process, as the highest energy electrons from the donor (located in the LUMO) and the acceptor (located in the HOMO) are exchanged. Since the acceptor gains an electron in its LUMO while giving up an electron from its HOMO, the acceptor becomes excited while conversely the donor is deactivated. While Dexter-type ET requires spectral overlap as in FRET, this process is also diffusion controlled and depends on the viscosity of the solvent (*i.e.* the environment) [19].

3 Ligand-Based Luminescence

3.1 Solid-State Luminescence of Organic Molecules

The study of luminescence from organic compounds in the solid state is of increasingly high importance. Besides the interest in fundamental physical studies, implementation of organic materials as active components in solid-state devices has led to increased attention in this area. Relevant examples include organic light-emitting diodes (OLEDs), thin-film sensors, and solid-state lasers. A major challenge for the development of such devices is suitable control over the morphology and interfacial properties of emissive organic species during device fabrication. Factors such as luminophore orientation, intermolecular distance, packing density, and details of the local molecular environment often have a significant impact on the resulting emission (and absorption) wavelength, intensity, and lifetime. Highly fluorescent organic molecules often feature an extended π-conjugated system (although this is not a requirement for emissive behavior). Such molecules share features in common with ligands often used in the field of metal-organic frameworks (MOFs), whereby a rigid, π-conjugated "linker" often is used to form the struts connecting metal ions or clusters. The overall structure of a MOF is mainly determined by geometric requirements arising from the strong coordination between the metal ions or clusters and the ligand groups, and may be varied by choosing suitable starting materials and/or growth conditions. MOFs, therefore, have a degree of structural predictability and can allow for a controllable platform for arranging luminophores in order to alter the solid-state emission properties of the material. Conversely, the structure of an entirely organic solid-state material (*i.e.*, a molecular solid) is often dictated by a multitude of weaker crystal packing interactions, including π–π stacking and hydrogen bonding, and there is little control over the structure ultimately formed in the solid state. For MOFs, the wide variety of organic ligands and coordination geometries available to afford predictable structures, as well as the ability to accommodate guests, potentially allows for many degrees of freedom and, consequently, rational modulation of the emissive properties of the material.

Several possibilities exist for the type of emission displayed by MOFs containing π-conjugated ligands. In some cases, there is little or no electronic interaction between the organic and inorganic moieties, leading to ligand-based luminescence, as will be discussed in Section 3.2. These ligands may be isolated from each other in the structure, resulting in emission

characteristic of a dilute solution of the free ligand, or the intermolecular distance and/or orientation may be such that significant interaction occurs, leading to ligand-to-ligand charge transfer (LLCT) emission with a typically broadened and red-shifted emission profile. Sections 3.3 and 3.4 describe materials for which the luminescence properties are determined not only by the organic molecule(s), but also through interaction with the metal unit(s). Two limiting cases are possible, ligand-to-metal charge transfer (LMCT) or metal-to-ligand charge transfer (MLCT). The particular type of emission observed depends on the structure of the MOF (which dictates spacing and orientation between the ligands and metal units), the electronic configuration of the metal, and the degree of orbital overlap between the organic and inorganic moieties. Several detailed structure-property relationships have been described for luminescent MOFs, using both steady-state and time-resolved measurements, with the number of reports in this area increasing significantly over the past few years. The following sections are intended to exemplify the important features and principles involved for correlating structure with observed luminescence in MOF materials.

3.2 Ligand-Based Luminescence in MOFs

Ligand-centered luminescence typically occurs for MOFs in which there is little-to-no electronic interaction between the organic and inorganic portions of the structure. Typically, this is the case for structures containing metal ions that have no *d-d* or *f-f* transitions possible, most commonly for MOFs with d^{10} Cd^{II}, Zn^{II}, and Ag^{I} ions. An excellent example of this is provided by the IRMOF series of Yaghi *et al.* [20], in which the bonding between anionic carboxylate linkers and Zn^{II} ions is essentially ionic and involves very little charge transfer (see discussion below). However, the presence of a d^{10} metal ion does not necessarily dictate that the structure will display ligand-based emission, as upon light absorption, the ligand may facilitate charge transfer to higher energy, emissive metal states if the ligand HOMO–LUMO gap is large. Moreover, as will be seen throughout this chapter, the complexity of MOF structures can frequently produce unexpected luminescent features that defy placement within straightforward categories such as this.

The IRMOFs illustrate the effect of increasing linker conjugation. When this occurs, the π–π^* energy gap decreases [13], making energy transfer to the metal less efficient. The resulting ligand-based emission resembles that of the corresponding ligand in dilute solution (Figure 2). A variety of IRMOFs exhibit emission similar to their isolated ligands, including IRMOF-11 $[Zn_4O(4,5,9,10\text{-tetrahydropyrene-}2,7\text{-dicarboxylate})_3]_n$, IRMOF-13 $[Zn_4O(2,7\text{-pyrene-dicarboxylate})_3]_n$ and $[Zn_4O(4,4'\text{-stilbene-dicarboxylate})_3]_n$ [1]. Each of these structures exhibits emission similar to that of the corresponding dilute ligand in solution, indicating ligand-centered luminescence dominates and there is little influence of the zinc Zn_4O cluster on the electronic structure of the ligand. In addition, the absence of other bands to the red of this emission indicates there is no *significant* LLCT.

A second factor that strongly influences ligand-based MOF emission is the possibility of interpenetration within the structure. The three IRMOF structures just discussed consist of interpenetrated frameworks as a consequence of the increased length of the rigid, linear linker. MOFs with interpenetrated structures consist of two or more frameworks intertwined, and details of the structure, such as distance between the interpenetrated frameworks and dihedral angle of the organic ligands, will lead to variations observed in the emission wavelength, fine-structure, and intensity. Although significant LLCT was ruled out by detailed experimental studies in the $[Zn_4O(4,4'\text{-stilbene-dicarboxylate})]_n$ structure [21] (as discussed in more detail below), this may

not necessarily be the case for other interpenetrated MOFs, such as the pyrene and tetrahydropyrene-based IRMOFs, for which careful studies of these two structures have not yet been carried out. However, other IRMOFs that exist as interpenetrated and non-interpenetrated versions have been probed in more detail. Meek *et al.* compared the excitation and emission spectra of the interpenetrated and non-interpenetrated versions of two IRMOFs constructed from the same ligand [22]. IRMOFs -9 and -10 are constructed from 4,4□-biphenyl dicarboxylic acid (with IRMOF-9 being interpenetrated), and IRMOFs -15 and -16 are constructed from 4,4□-terphenyl dicarboxylic acid (IRMOF-15 is interpenetrated). In the terphenyl MOFs, the interpenetrated structure exhibits red-shifted emission when compared to the non-interpenetrated variant, suggesting that interpenetration induces greater charge transfer, possibly due to smaller linker-linker and linker-metal distances. In the biphenyl structures, the interpenetrated MOF (IRMOF-9) displays a completely new band at ~ 500 nm, indicating formation of a new excited state. This emission is broad and unstructured, suggesting that it involves charge transfer between biphenyl linkers in close proximity.

One might ask why this section did not begin with a discussion of IRMOF-1, the simplest of the cubic IRMOF structures, in which the linker is 1,4-BDC(1,4-benzene dicarboxylate) [23]. Here, although the BDC linker is fully conjugated, the HOMO-LUMO energy gap is large; the excitation maximum of the isolated linker in dilute DMSO solution occurs at 338 nm. In contrast, a green emission upon UV excitation is observed from IRMOF-1 in some cases. This has been attributed to an LMCT process, whereby energy transfer occurs from the 1,4-BDC singlet excited state to the Zn_4O clusters [23]. Although this mechanism is supported by excitation spectra indicating that light absorption occurs *via* the benzene unit and by *ab initio* studies [24], recent work demonstrates that ligand-centered luminescence is actually the dominant process and that the green emission attributed to LMCT is due to synthetic byproducts present in the structure or degradation of the structure itself (framework collapse) [25]. This investigation emphasizes that unambiguous knowledge of the structure and constituents (including contaminants) of a material is necessary for accurate interpretation of the physical causes behind observed luminescence properties. Additionally, it demonstrates that changes in framework structure, undetectable by standard characterization methods such as powder X-ray diffraction, can be easily identifiable by the significantly more sensitive luminescent methods.

Figure 2.

The effects on the emission properties of varying the orientation and spacing between ligands have also been demonstrated in the case of Zn stilbene MOFs [21]. Two MOF structures with different topologies were synthesized from the same starting materials *via* changes in the growth conditions and solvent, yielding both a 2-periodic net $[Zn_3\mathbf{L}_3DMF_2]_n$ and a cubic 3-periodic framework $[Zn_4O\mathbf{L}_3]_n$ structure, where **L** = 4,4'-stilbene dicarboxylate (Figure 3). Both materials exhibit intense ligand-based luminescence, similar in shape and vibronic structure, signifying little to no influence of the different metal cluster types present in each structure. However, emission from the 2-periodic structure is red-shifted and broadened from that of the cubic 3-periodic structure, indicating a greater degree of interaction between luminophores in the 2-periodic structure. This is consistent with the 6.0 Å, cofacial spacing between ligands in successive layers observed for this structure. It should be noted that the extent of this intermolecular interaction is small compared to that observed for the ligand itself in the solid state, which exhibits a significantly broader and red-shifted emission. The 3-periodic cubic

structure consists of anisotropically-catenated cubes (edges are closer along the *b*-axis), a likely result of very moderate stilbene-stilbene interactions. The closest linkers are not cofacial in these structures, but rather tilted with a 49° dihedral angle with respect to one another. In this case, the MOF exhibits luminescence similar to a dilute solution of the ligand, a situation where LLCT is minimal.

Figure 3.

An additional point of interest, exemplified by the stilbene MOF structures just discussed, is that the MOF materials often display increased emission intensity when compared to the ligand itself. In the framework structures, the stilbene units are held tightly through strong metal coordination, and their motion is restricted. This inhibits the non-radiative *cis–trans* isomerization process that occurs readily for stilbene in solution upon absorption of light, and results in a concomitant increase in the fluorescence intensity of the rigidified ligand in the MOFs [26-27]. An increase in the radiative lifetime typically leads to an increase in the fluorescence quantum yield by reducing the efficiency of such non-radiative pathways. Bi-exponential emission decay was observed for the 2-periodic Zn stilbene structure, consistent with two emission pathways for the stilbene (*i.e.*, isolated ligand-based emission and LLCT). However, the lower density cubic Zn stilbene MOF exhibited mono-exponential emission decay (consistent with isolated stilbene units), with a 0.50 ns lifetime, approximately 5 times larger than for stilbene in solution. The increase in lifetime is indicative of the rigidity provided by incorporation into the MOF structure. As minor structural changes can lead to observable changes in luminescence properties, this allows for a natural extension of ligand-based luminescence into the field of sensing (Section 6). For instance, upon changing the guest solvent molecules in the cubic Zn stilbene MOF, the emission is found to shift in wavelength. This may be a result of a change in local dielectric environment for the ligand or minor changes in the overall framework structure, such as expansion or compression of the catenated units.

As luminescence can be extremely sensitive to local environment, the study of spectral properties has become a standard method for materials characterization as it is a simple, rapid indicator of structural changes and/or maintenance of structural integrity after MOFs have been subjected to a new environment. For example, recent work has shown that the ethylene bridge of stilbene in the 3-periodic cubic Zn MOFs can be partially brominated without collapsing the structure [28]. However, full bromination interrupts the interpenetrated cubic units, leading to partial collapse, as was quickly determined by measurement of the luminescence spectra (revealing a broadened, red-shifted spectrum) and later verified *via* detailed structural studies. Another interesting aspect, supported by luminescence studies, is the change in stability to evacuation between structures upon bromination. As-prepared stilbene zinc 3-periodic MOFs do not maintain their structure after full evacuation, a likely result of a change in the π–π interactions between interpenetrated cubes, which alter the stilbene-stilbene distance and disturbs the structure. This leads to lower-than-expected surface areas (560 m^2/g) and a weakened, red-shifted luminescence with loss of vibronic structure upon evacuation (see Figure 4). However, after partial bromination, the inter-cube attractions are reduced and the structure remains intact upon evacuation, with an observed increase in surface area (1600 m^2/g) despite the fact that the bromine atoms occupy some of the pore space. The emission spectrum of these partially-brominated MOFs is nearly unperturbed from that of the as-prepared 3-periodic material before evacuation or bromination, as shown in Figure 4 (presumably, the brominated stilbene units are substantially quenched and do not significantly contribute to the spectra).

Figure 4.

A recent study by Rosseinsky and co-workers also clearly demonstrates the direct influence of local ligand environment on the overall emission characteristics for MOF materials based on a luminescent pyrene core, $[In_2(OH)_2(TBAPy)]_n$ (TBAPy = 1,3,6,8-tetrakis(*p*-benzoic acid)pyrene) [29]. The $TBAPyH_4$ ligand itself exhibits an emission lifetime of 89 μs, which increases to 110 μs upon incorporation into the MOF, attributed to rigidification. Bright blue luminescence is observed upon coordination of the ligand in the MOF (see Figure 5), with a blue shift of 66 nm from that of the free ligand due a reduction of LLCT through isolation of the ligands from one another in the framework. Interestingly, upon evacuation of guest DMF molecules, the emission red-shifts, the quantum yield decreases, and the fluorescence lifetime decreases. This is a direct result of the structural distortion which increases the degree of through-space coupling of the pyrene cores, elegantly demonstrated by single crystal diffraction studies. Upon resolvation with DMF, the original structure and luminescence properties are restored. Altering the identity of the guest molecules is also found to cause a change in emission, as will be discussed in Section 6.1.1. Other cases of luminescence enhancement due to the rigid environment in MOFs have also been reported [30-33].

Figure 5.

3.3 Ligand-to-Metal Charge Transfer in MOFs

LMCT-based emission is often reported for Zn^{II} and Cd^{II} MOFs when the sufficiently absorptive ligand has a relatively large HOMO-LUMO gap (as discussed in the previous section), leading to significantly red-shifted emission when compared to the ligand itself. Many MOFs displaying LMCT emission contain BDC linkers, benzene tricarboxylic acid (BTC), or both ligands [34-37]. In these cases, green emission is associated with UV excitation and assigned to a LMCT. However, as discussed above, this may be a consequence of an impurity (possibly ZnO). Often, ligand-based luminescence competes with LMCT, and both cases can be observed under certain circumstances. For example, $[Zn_3(1,4\text{-BDC})_2(1,3,5\text{-BTC})_2(NH(CH_3)_2)(NH_2(CH_3)_2)_2]_n$, emits at 430 nm due to LMCT, with a shoulder at 370 nm arising from emission from the BTC ligand [34]. There are also reported examples of LMCT from MOFs containing ligands other than BDC and BTC. Subtle variations in the environment can alter the efficiency of energy transfer from the ligand to the metal center, as described by Huang *et al.* for Cd^{II} 2,6-di-(4-triazolyl)pyridine-based MOFs [38]. Ligand-based luminescence is observed for the hydrated structure, a result of water in the lattice preventing efficient charge transfer. However, the emission gains significant LMCT character upon dehydration as the charge transfer process dominates.

The efficiency of LMCT is a function of the orbital overlap between ligand and metal and therefore, the observation of ligand-based luminescence *vs*. LMCT can also depend on the type of metal center. A recent study of 18 MOF structures containing tetrapyridyl ligands bound to either Zn^{II}, Cd^{II}, or Hg^{II} metal centers demonstrates how subtle variations in the structure can alter the emission character [39]. These materials emit in a multitude of colors, from violet to yellow, depending on the structure type and metal ion. The luminescence intensity for all of the Zn^{II} and Cd^{II} structures was enhanced compared to the free ligand due to the rigidity afforded by coordination in the MOF structure. However, the Hg^{II} structures display reduced emission intensity, attributed to a heavy-metal quenching effect.

In another interesting recent study, the photoluminescence spectra of three structures

containing Cd^{II}, 4,4′-bipyridine, and 2-amino-1,4-BDC were found to be characteristic of either a mixture of LMCT and ligand-centered emission, or only LMCT [40]. Upon desolvation and framework distortion, LMCT character is quenched, while ligand-centered luminescence grows in. Main-group metal complexes may also display LMCT in certain cases, for example $[Pb_4(1,3\text{-}BDC)_3(\mu_4\text{-}O)(H_2O)]_n$ exhibits a strong emission peak at 424 nm originating from LMCT between delocalized π-bonds of the BDC groups and *p*-orbitals of the Pb^{II} ions [41].

3.4 Metal-to-Ligand Charge Transfer in MOFs

MLCT is less commonly reported for MOFs than LMCT, and is typically observed for d^{10} Cu^{I} and Ag^{I}-based MOFs where there is the possibility of *d*-electron transfer into low-lying empty ligand states (*e.g.*, for π-acid ligands). For example, N-heterocylic-based Cu(I) MOFs displaying a multitude of geometries were shown to luminesce with varying degrees of intensity [42], (assigned to a Cu→CN MLCT process), and $[Cu(1,2,4\text{-}BTC)(2,2\text{-}bipyridine)]_n$ was found to exhibit intense blue MLCT emission with a lifetime of 13.62 ns [43]. These mixed-valence complexes also exhibit intervalence charge transfer (IVCT).

Excitation of the 2-periodic layered MOF $[Ag(4\text{-}(2\text{-}pyrimidylthiomethyl)benzoic\ acid)]_n$ at λ = 370 nm results in an intense green emission with peak maximum at 530 nm, the origin of which was assigned to LMCT and/or MLCT modified by metal-centered (*ds*/*dp*) states mediated through Ag-Ag interactions [44]. Similarly, $\{[Ag(4,4'\text{-}bipyridyl)][Ag(1,2,4\text{-}HBTC)]\}_n$ exhibits an intense emission band with a maximum at 502 nm (λ_{ex} = 410 nm) due to MLCT [43].

4 Metal-Based Luminescence

4.1 Metal Luminophores

When discussing metal ions and their salts, only the rare earth elements and some uranyl compounds are typically luminescent. For example, all of the lanthanide trivalent ions (Ln^{III}) except for La^{III} and Lu^{III} are luminescent and their emissions span the spectrum from UV (Gd^{III}) to the visible (Pr^{III}, Sm^{III}, Eu^{III}, TB^{III}, Dy^{III}, and Tm^{III}) to the near-IR (NIR; PR^{III}, Nd^{III}, Ho^{III}, Er^{III}, and Yb^{III}) [45]. Some of these elements are fluorescent, while others exhibit phosphorescence, although in some instances they can exhibit both fluorescence and phosphorescence. For compounds composed of uranium, only the U^{VI} uranyl ion $[UO_2]^{2+}$ is fluorescent and typically emits in the range of 520–620 nm.

4.2 Lanthanide Luminescence and the Antenna Effect

Trivalent lanthanide ions (Ln^{III}) are attractive luminophores because they exhibit spectrally narrow emission with long lifetimes in the solid state and in solution [46]. The 4*f* orbital is shielded by a filled $5s^25p^6$ sub-shell, thus screening the inner-shell 4*f*-4*f* electronic transitions which generate well-defined energy gaps for the electronic levels allowing for the line-like emission. However, electronic transitions for Ln^{III} ions are formally forbidden by parity selection rules (Laporte's rule), typically leading to weak absorbance and, therefore, low brightness. One method of overcoming the weak absorption cross-sections of these ions has been to complex them with strongly absorbing organic molecules. Additionally, complexation often prevents quenching of luminescence by solvent molecules. When efficient vibronic coupling exists

between the organic ligand and Ln^{III} moieties, direct energy transfer from the organic molecules' excited state to the metals' elevated energy levels is possible (Fig 6). This coupling, first identified by Weissman in 1942, leads to a large increase in luminescence intensity and is widely known as the "antenna" effect or "luminescence sensitization" [45,47]. For Ln^{III} ions the electronic dipole transitions are of the same order of magnitude as that of the magnetic dipole transitions, and thus both are readily seen in the optical spectra.

Figure 6.

4.3 Examples of Metal-Based Luminescence

4.3.1 Metal-Centered Luminescence

Many isostructural series of Ln^{III}-containing MOFs are known; however, typically, only the luminescence properties of the Eu^{III} and Tb^{III} analogues are reported [48-60]. The likely reason these two metals predominate luminescence reports is two-fold: they benefit from strong coupling to most organic ligands used for MOF synthesis (antenna effect) and their red and green emission in the visible range is easier to detect with common laboratory equipment when compared with the longer wavelength emission of several other Ln^{III} ions. In complexes comprised of Eu^{III}, the $^5D_0 \rightarrow {}^7F_J$ transition series (J = 0 – 4) is the most readily observable, typically with the $J = 1$ and 2 transitions being both the strongest and most useful for structural determination and sensing. The dominant emission of the $^5D_0 \rightarrow {}^7F_2$ transition usually occurs around 615 nm, leading to the brilliant red color characteristic of Eu^{III} luminescence. The emissions observed for Tb^{III} come from the $^5D_4 \rightarrow {}^7F_J$ transitions (J = 3 – 6), with the strongest typically being that of $J = 5$ and 6 and giving rise to the strong green luminescence in the 540–555 nm range characteristic of Tb^{III} complexes.

An illustrative example of metal-centered luminescence was provided by Li *et al.,* wherein they report a series of Ln^{III}- MOFs based upon $[Ln_4(OH)_4]^{8+}$ cubane-like SBUs [61]. The structures, which have unit formula $\{[Ln_4(OH)_4(3\text{-SBA})_4(H_2O)_4]\bullet nH_2O\}_n$, (Ln = Eu^{III} (**1**), Gd^{III} (**2**), Tb^{III} (**3**); 3-SBA = 3-sulfobenzoate), are 3-periodic porous frameworks with unique (3,12) topology. The PL of **1** and **3** is characteristic of Ln^{III} metal-centered luminescence. The excitation spectra of **1**, monitored at the strongest Eu^{III} transition ($^5D_0 \rightarrow {}^7F_2$; 614 nm), displays an intense, broad band centered at 286 nm that was attributed to the ligand centered $\pi \rightarrow \pi^*$ transition, as well as several much weaker narrow bands attributed to direct *f-f* transitions within the Eu^{III} metal center ($^7F_0 \rightarrow {}^5H_4$, 318 nm; $^7F_0 \rightarrow {}^5G_6$, 362 nm; $^7F_0 \rightarrow {}^5G_{0\text{-}4}$, 377–382 nm; $^7F_0 \rightarrow {}^5L_6$, 395 nm; $^7F_0 \rightarrow {}^5D_3$, 416 nm). The emission spectra of **1** (λ_{ex} = 286 nm) exhibit several narrow spectral lines assigned as $^5D_0 \rightarrow {}^7F_J$ (J = 0–4) and dominated by the hypersensitive $J = 2$ peak at 614 nm, resulting in bright red luminescence. No emission corresponding to the $\pi^* \rightarrow \pi$ transition of the ligand is observed, indicating that the fluorescence is entirely metal-centered emission. The lifetime of the $^5D_0$ state was also determined to be τ = 0.135 ms, based upon the strongest transition. In the case of **3**, the excitation spectrum was monitored at 545 nm ($^5D_4 \rightarrow {}^7F_5$) and again a strong absorption band at 288 nm was observed and assigned as the $\pi \rightarrow \pi^*$ transition. Additionally, the significantly weaker *f-f* transitions for Tb^{III} were also present ($^5G_2$, 351 nm; $^5D_3$, 359 nm; $^5D_2$, 369 nm; $^5D_4$, 377 nm). The emission spectra (λ_{ex} = 350 nm) of **3** is dominated by the hypersensitive $^5D_4 \rightarrow {}^7F_5$ (545 nm with a shoulder at 549 nm), but also displays the remaining transitions from the lowest excited state to the ground state manifold ($^5D_4 \rightarrow {}^7F_{6\text{-}3}$: J = 6, 489 nm; $J = 4$, 528–590 nm; $J = 3$, 622 nm). The lifetime for the $^5D_4$ state was observed to be τ = 1.035 ms.

In another example of metal-centered emission, Choi *et al.* describe electron transfer and size-selective electron oxidation of organic compounds by a MOF based on Eu^{III} and 1,3,5-benzenetribenzoate [62]. When the ligand is selectively excited (λ_{ex} = 285 nm), the MOF displays characteristic Eu^{III} luminescence, emitting narrow line shapes at wavelengths attributed to $^5D_0 \rightarrow {}^7F_J$ (J = 1, 2, 3, 4; 593, 615, 653, 698 nm) with no observable emission from the ligand. This suggests efficient LMCT and metal-centered emission. The authors investigated this material for the ability to facilitate electron transfer from the organic moieties to the Eu^{III} metal ions. Upon irradiation of the MOF, while in the presence of an acetonitrile solution of N,N,N□,N□-tetramethyl-*p*-phenylenediamine (TMPD), with strong UV light (365 nm; 50 mW cm^{-1}; 10 min), the solution turned deep blue, indicative of the formation of the oxidized $TMPD^{\bullet+}$. This material also showed strong absorption at 565 nm and 614 nm after irradiation, both in good agreement with the presence of $TMPD^{\bullet+}$. Furthermore, the authors report size-selective one electron oxidation of several other organic compounds together with detailed experimental (time-resolved absorption and emission spectroscopy; confocal microscopy) and theoretical observations (Marcus theory calculations).

An interesting *solvatochromic effect* is reported by Lin *et al.* and provides another example of metal-centered luminescence. These authors describe a series of porous 3-periodic Ln^{III}-MOFs [63], $\{[Ln_4(BPT)_4(DMF)_2(H_2O)_8]\bullet(DMF)_5\bullet(H_2O)_3\}_n$, ($H_3BPT$ = biphenyl-3,4□,5-tricarboxylic acid; Ln = Eu (**1**), Gd (**2**), Tb (**3**), Dy (**4**), Ho (**5**) or Er (**6**)). The ligand H_3BPT was specifically targeted because it was expected to strongly absorb UV light and act as a good sensitizer of Ln^{III} ions, and because other multi-carboxylate organic molecules afford extended architectures when coordinated to Ln^{III} ions. Compound **4** displays no observable fluorescence when excited using UV radiation; however compounds **1** and **3** exhibit characteristic red and turquoise emissions respectively. The emission of the $\pi^* \rightarrow \pi$ transition seen in the emission spectrum of the isolated ligand (λ_{ex} = 300 nm) was not observed for either of the MOF compounds, suggesting efficient sensitization and metal-centered luminescence. Again, the dominant peaks were attributed to the so-called hypersensitive transitions: $^5D_0 \rightarrow {}^7F_2$ (617 nm) in the case of Eu^{III} and $^5D_4 \rightarrow {}^7F_5$ (544 nm) for the Tb^{III} compound. Quantum yields were also obtained for these two compounds with Φ_1 = 0.1442 and Φ_2 = 0.6087 obtained for the Eu^{III} and Tb^{III} MOFs, respectively. The rather high value for the Tb MOF is quite surprising, particularly given the presence of nine coordinated water molecules, which one would expect would quench the Ln^{III} luminescence. The compounds were annealed in air at 220 °C for four hours, causing the quantum yields to unexpectedly *decrease* (Φ_{1A} = 0.052; Φ_{2A} = 0.326). The initial quantum yields are only partially recovered upon rehydration (Φ_{1B} = 0.12; Φ_{2B} = 0.582), suggesting a possible irreversible change in the compounds upon dehydration and subsequent rehydration. The variation in PL for the as-synthesized, dehydrated, and re-hydrated forms of these two Ln-MOFs suggests a possible solvatochromic effect in these materials, which is counter to the commonly understood phenomenon of water-quenched luminescence.

The efficiency of energy transfer from absorbing linkers to lanthanide ions within MOFs is not uniform, as shown by a detailed analysis conducted by Soares-Santos *et al.* These investigators measured the PL of a series of Ln^{III} MOFs, showing that Eu^{III} and Tb^{III} are more efficiently sensitized than their Nd^{III} and Sm^{III} counterparts [64]. In this investigation, 2,3-pyrazinedicarboxylate (2,3-pzdc) and oxalate (ox) combine with Ln^{III} ions to generate 2-periodic bilayer structures with unit formula $[Ln_2(2,3\text{-pzdc})_2(ox)(H_2O)_2]_n$, (Ln = Ce, Nd, Sm, Eu, Gd, Tb or Er). In this structure, individual cationic layers interconnect *via* ox^{2-}. In the Nd^{III} and Sm^{III} cases, the more intense spectral peaks (Nd: $^4F_{3/2} \rightarrow {}^4I_{11/2}$; Sm: $^4G_{5/2} \rightarrow {}^6H_{9/2}$) were used to monitor

the excitation; several narrow peaks corresponding to transitions from the ground states (Nd: $^4I_{9/2}$; Sm: $^6H_{5/2}$) to higher energy levels were observed. Additionally, intense, broad absorption bands from 250–400 nm attributed to ligand $\pi \rightarrow \pi^*$ transitions are observed for both MOFs. This ligand absorption is stronger than for the metal transitions, suggesting more efficient sensitization *via* ligand excited states than for direct excitation of metal transitions. The emission spectra for both the Nd^{III} and Sm^{III} compounds were characteristic of their Ln^{III} ions, with emissions in the NIR (*e.g.* for the Nd^{III} compound the strongest observed peak was for $^4F_{3/2} \rightarrow {}^4I_{11/2}$ at 1064 nm). However, both of these compounds also exhibit large and broad emission bands from 380–540 nm, indicative of $\pi^* \rightarrow \pi$ emission from the ligands, suggesting incomplete LMCT. In the case of Gd^{III}, the excited energy levels of the metal ions are higher than that of the S_n or T_n energy levels of the ligand, precluding the possibility of energy transfer from the ligand to the metals. As such, the emission for this compound was attributed solely to the two ligands, and through detailed analysis the authors were able to determine that the emissions are due to the excited triplet states of the two ligands. Additionally, they determined the relative energies for the two triplet states and deduce that the 2,3-pzdc is a better sensitizer than the oxalate. In the case of the Tb^{III} and Eu^{III} compounds PL similar to the other materials described in this section is observed. The excitation spectra exhibit intense, broad brands attributed to $\pi \rightarrow \pi^*$ transitions centered on the ligands as well as weaker and much more narrow peaks assigned to transitions from the ground state to higher energy excited states for the Ln^{III} ions, while the emission spectra are characteristic of the respective Ln^{III} ions and show no observable transitions from the ligands. This suggests that either the efficiency of ligand-to-metal energy transfer is higher in the cases of Tb^{III} and Eu^{III} than those of Nd^{III} and Sm^{III}, or that there is some non-radiative deactivation of ligand excited states in the former two cases not observed in the latter.

As a final example of metal-centered luminescence, Li *et al.* describe a group of MOF materials in which LMCT can be essentially "switched off" and either ligand-centered or metal-centered emission is observed based on the selection of metal ion. The authors report a series of MOFs constructed from the same ligand, 2-(pyridine-4-yl)-1*H*-imidazole-4,5-dicarboxylic acid (H_3PIDC), but with lanthanide or non-lanthanide metal ions (Fe^{II}, Cd^{II}, Zn^{II}, Eu^{III}, Tb^{III} and Y^{III}) [65]. In the compounds comprised of Cd^{II}, Zn^{II} and Y^{III}, the observed emission is broad and slightly blue-shifted relative to the free ligand, suggesting only ligand-centered emission. However, in the compounds containing Tb^{III} and Eu^{III}, no broad ligand-centered emission is observed, while sharp, narrow emissions characteristic of the Ln^{III} ion are detected. In this study, we see that the presence of Ln^{III} ions enables efficient LMCT, preventing the $\pi^* \rightarrow \pi$ intraligand transitions while at the same time generating metal-based excited states, leading to Ln^{III} emission. When the Ln^{III} ions are replaced with d^{10} metals, no LMCT occurs and the PL is attributed solely to ligand-centered emission.

4.3.2 Metal-to-Metal Charge Transfer (MMCT)

The potential for energy transfer between metals within a MOF also exists. In one report, two isostructural 4,4'-bipy templated frameworks were prepared using Tb^{III} and 1:1 Eu^{III}:Tb^{III} [66]. Both of these structures exhibit efficient through-space sensitized luminescence originating from the lanthanide centers. However the compounds containing Eu^{III}:Tb^{III} show greater sensitization efficiency than the structure comprised solely of Eu^{III}. The quantum yields for the materials were reported to be $\Phi_{Eu} \approx 0.22$ and $\Phi_{Tb} \approx 0.32$. Perhaps even more interesting, the mixed-metal MOF

exhibits a metal-to-metal antenna effect in which the luminescence expected from the Tb^{III} luminophore is nearly completely quenched, leaving an emission spectrum for the material dominated by the Eu^{III} luminophore. Due to the absence of the Tb^{III} emission, as well as the increased quantum yield ($\Phi_{Eu/Tb} \approx 0.39$ compared to $\Phi_{Tb} \approx 0.32$), it is likely that energy transfer from the higher energy Tb^{III} $^5D_4$ state to the Eu^{III} $^5D_0$ state occurs.

Metal-to-metal charge transfer could also be useful as a structural probe. Soares-Santos *et al.* describe a series of mixed-ligand lanthanoid frameworks constructed from 2,5-pyridinedicarboxylate and 1,4-phenylenediacetate along with Eu^{III}, Tb^{III}, and two non-equivalent mixtures of Eu^{III} and Tb^{III} [67] Each of these MOFs demonstrates sensitized metal-centered luminescence through an antenna effect, while the mixed-metal MOFs exhibit Tb^{III}-to-Eu^{III} MMCT. In the mixed-metal frameworks, this energy transfer can serve as a structural probe by indicating the extent of metal ion dispersal throughout the material. MOFs having single-metal ion clusters would be expected to exhibit very little of this Tb^{III}-to-Eu^{III} MMCT. Conversely, when the metal ions are homogeneously dispersed throughout the structure, the Tb^{III}-to-Eu^{III} MMCT should be efficient and easily observed.

4.4 Lanthanide Luminescence as a Probe of the Metal-Ligand Coordination Sphere

An illustrative example of how lanthanide luminescence can be used as a structural probe of the metal-ligand coordination sphere is that of Eu^{III}. The ratio of relative intensities for the $^5D_0 \rightarrow {}^7F_J$ ($J = 2$:$J = 1$) transitions is very sensitive to the site symmetry of the Eu^{III} centers. Since the electric dipole transition ($J = 2$) is hypersensitive to the ligand environment while the magnetic dipole transition ($J = 1$) is practically insensitive, it is sometimes possible to elucidate some aspects of symmetry for the material even in the absence of other structural data [68]. This effect is also observed in Ln-based MOFs, particularly a Eu^{III} -doped version of MIL-78 [69], an open framework structure comprised of one-periodic inorganic columns of eight-coordinate polyhedra connected by bridging trimesate linkers. Luminescence data depict a nearly equivalent intensity for the $^5D_0 \rightarrow {}^7F_2$ and $^5D_0 \rightarrow {}^7F_1$ transitions ($^7F_2$:$^7F_1 \approx 1$), suggesting that the Eu^{III} ions lie in an environment of high symmetry relative to the ligand, which was independently confirmed by single-crystal X-ray diffraction data. In another example, a MOF structure exhibiting chirality shows the ability of Ln^{III} luminescence to be used as a structural probe. Yue *et al.* synthesized a group of homochiral Ln-phosphonate frameworks with the enantiomerically pure ligand *s*-*N*-(phosphonomethyl)proline and several lanthanide ions (Ln = Tb, Dy, Eu, Gd)[59]. The chirality of the MOF arises from the chiral organic ligand, leading to a MOF structure comprised of a series of 1-periodic triple-stranded helices. PL spectra for both the Tb^{III} and Eu^{III} analogues exhibit significant splitting in the $^5D_4 \rightarrow {}^7F_J$ series ($J = 6$–4), indicative of a strong crystal field that results from the asymmetric environment of the metal center. While symmetric systems often have forbidden transitions, the asymmetry inherent in these MOF structures leads to high intensity ratios for the $^7F_2$:$^7F_1$ transitions, as well $^7F_0$ transitions that are more intense than even the $^7F_1$ transition, an unusual happenstance.

5 Guest-Induced Luminescence

In the previous two sections we have discussed the phenomenon of luminescence as it arises directly from the metal-organic framework itself, either from the organic linker or the inorganic cluster. However, many MOFs have periodic scaffolds that generate well-defined, essentially permanent, nanopores and large free-volume cavities. These unfilled cavities of controllable size

enable encapsulation of a wide variety of guest molecules. In relation to MOF-based luminescence properties, the ability to encapsulate guest molecules could prove useful in a number of ways. For instance, a non-luminescent MOF could be infiltrated with a luminescent guest molecule, which lends luminescent properties to the hybrid MOF-guest material, thereby imparting desired luminescent properties into the MOF. It may also be possible that upon infiltration of the MOF, a new luminescent species is formed through MOF-guest interactions (*e.g.* exciplex) with different luminescence properties from that of either the pristine MOF or guest molecules by themselves. In this case, both the MOF and guest may or may not be luminescent on their own, but upon complexation they generate a new species capable of luminescence. Additionally, the inclusion of a guest molecule could lead to modulation of the inherent luminescence of the MOF host. It may then be possible to enhance (or quench) the luminescence of the MOF by incorporating specific guest molecules, thereby allowing the MOF to act as a sensor.

5.1 Encapsulation of Luminophores

Conceptually, the infiltration of a porous, non-luminescent MOF with a luminescent guest molecule is the simplest way of introducing desired luminescence properties in a MOF material. Müller *et al.* synthesized a selection of well-studied MOFs (MOF-5, MOF-177, UMCM-1, and MIL-53Al) and investigated the ability to incorporate strongly luminescent guest molecules into these frameworks *via* the vapor phase [70]. The luminophores they chose were N,N-bis(2,6-dimethylphenyl)-3,4,9,10-perylene tetracarboxylic diimide (DXP) and (2-carboxypyridyl)bis(3,5-difluoro-2(2-pyridyl)phenyl)iridium(III) (F_2-ppy), and in each case, the infiltrated MOF exhibits PL spectra dominated by the luminophore guest. The authors attempted to remove the luminophores by washing the hybrid materials and observed that, for the F_2-ppy compounds, partial-to-total removal was possible, coupled with decreases in PL intensity. However, removal of DXP was not achieved, possibly indicating stronger interactions with the frameworks. The emissive properties of the DXP-MOFs suggest host-guest interactions such as caging effects, aggregate formation, and strong quenching of the MOF host luminescence.

In another example, this time involving infiltration of charged dye molecules, Zhang *et al.* report synthesizing nanoscale Ln^{III} MOFs (Ln = Gd, Eu, Yb) that exhibit temperature-controlled guest encapsulation and light harvesting [71]. The MOFs are constructed from highly conjugated linear linker molecules, and when the coordination spheres of the Ln^{III} ions are filled with non-bridging anions such as acetate, the lanthanide clusters are negatively charged. This allows infiltration of the MOFs with cationic dye molecules (*trans*-4-styryl-1-methyl pyridiniumiodide and methylene blue), upon which the MOF-based luminescence is quenched and FRET emission is observed. The intensity and efficiency of FRET is controllable based on the temperature of the MOF synthesis, which was shown to directly correlate with the percent loading of the guest luminophore. Interestingly, the dye and linker together in solution (DMF) demonstrated luminescence quenching, but no energy transfer, suggesting that the highly ordered arrangement of the dye guest molecules within the MOF cavities favor light harvesting. This study is significant, not only for the sequestration of a luminophore within the cavities, but also because it demonstrates that MOF-guest interactions can have profound effects on the resultant PL properties.

It is also possible to use the presence of a guest molecule to efficiently quench the luminescence of a MOF. Park *et al.* reported the structure and luminescence spectra of a mesoporous MOF derived from a superstructure of Tb^{III} ions, triazine-1,3,5-(4,4′,4″-

trisbenzoate), and dimethylacetamide [72]. The crystal structure reveals large pores (3.9 and 4.7 nm in diameter), and upon activation, the material shows a Langmuir surface area of 3855 m^2/g. PL studies demonstrate bright green, sensitized luminescence characteristic of the Tb^{III} ions. To investigate the potential for uptake of guest molecules, vapor phase ferrocene was introduced to the structure using elevated temperatures and reduced pressure. Figure 7 shows several transmission and fluorescence microscopy images, as well as luminescence spectra for the as-synthesized and ferrocene-containing framework. A color change of the single crystals from colorless to a dark brown, in addition to loss of Tb luminescence, are indicative of ferrocene inclusion. Additionally, the authors demonstrate that extraction of the ferrocene moieties is possible by using vacuum and high temperature, and that upon ferrocene removal, the framework luminescence is reestablished. Elemental analysis also indicated a high uptake of ferrocene within this MOF.

Figure 7.

5.2 Guest-Induced Charge Transfer: Excimers and Exciplexes

One way of introducing or modulating the luminescence of a MOF material is to generate an entirely new luminescent species in the form of an excited state complex. When the two molecules in question are the same they form a homodimer excited state complex or *excimer* (excited dimer). In the case where the two molecules are different, the excited state complex is a heterodimer called an *exciplex* (excited complex)[16]. Formation of exciplexes or excimers in MOFs is possible by two routes: 1) as a result of the framework structure itself or 2) by infiltration with a guest molecule. In the first possibility, the relative orientation of framework linkers allows the formation of an excited-state complex upon absorption of a photon. This could be achieved as a result of the framework topology itself; by 'breathing' in a flexible framework that alters the structure and brings the ligands into closer contact (and in the correct orientation); or by framework interpenetration, whereby the two linker molecules are contained on different nets, but located adjacent to one another. In the second possibility, infiltration of the framework with an appropriate guest molecule, and the subsequent interaction of this molecule with the ligands, could result in an excited state complex. In both the exciplex and the excimer, the effect on the observed luminescence is the formation of typically broad and featureless emission spectra, which is noticeably red-shifted in comparison to the individual monomer(s). The exciplex or excimer emission is highly dependent on the orientation of the component molecules, so that formation of these excited state species and observation of their PL can provide information not only on the presence of a guest molecule (sensor), but can also provide structural information regarding the interaction between the host and guest (structural probe). Cofacial arrangements of the two molecules are generally believed to be favorable to excimer and exciplex formation, while electronic structure modeling suggests the strength of the interaction is strongly dependent on the separation distance [73].

Exciplexes have only been reported in MOFs on a few occasions. Perhaps the most extensive investigation was conducted by Zaworotko and coworkers, who synthesized several MOFs in which aromatic molecules are intercalated within the framework to allow exciplex formation. In one case, 4,4'-bipyridine (4,4'-bipy) and pyrene form a 1-periodic molecular ladder coordination polymer with the unit formula $\{Zn(4,4'\text{-bipy})_{1.5}(NO_3)_2 \bullet CH_3OH \bullet 0.5\text{pyrene}\}_n$ in which the 4,4'-bipy linker assumes a cofacial arrangement with the intercalated pyrene molecule[74]. The pyrene moieties are not coordinated to the zinc ions, but rather trapped within the matrix to form

a 2:1 4,4'-bipy:pyrene exciplex. The ratio of relative intensity between the third and first peaks within the vibronic structure of the weak monomer fluorescence band for pyrene can be used as a probe for the polarity of the micro-environment surrounding the pyrene [16]. The results suggest the possibility of using both excimer formation and the emission of the monomer as an internal probe of adsorbed guest (solvent) molecules. In another example [75], this same group prepared a series of Zn^{II}-4,4'-bipy MOFs having 1-periodic ladder and 2-periodic square grid topologies. In these examples the nature of the aromatic solvent molecule (benzene, chlorobenzene, *o*-dichlorobenzene, *p*-xylene and toluene) determines the topology of the structure that results. Both λ_{max} and τ_F of the fluorescence are influenced by the structure. The emission of the 1-periodic structures is red-shifted ($\lambda_{max} \sim 520$ nm *vs.* 460 nm) in comparison to the 2-periodic emission and displays shorter lifetimes ($\tau_F \sim 43$ ns *vs.*74 ns). These features of the exciplex luminescence lead to a structural interpretation of face-to-face π–π stacking in the 1-periodic structures, but for an edge-to-face C-H···π interactions in the 2-periodic structure. This work is the most detailed analysis to date of the exciplex phenomenon in MOFs and demonstrates the way in which MOFs can be implemented as a platform to systematically perturb the identity and orientation of exciplex components. Conversely, the study also reveals how subtle changes in the MOF can lead to dramatic changes in the luminescence properties, demonstrating their potential use as good diagnostic handles for MOF structure.

Separately, another research group has demonstrated a case of guest-influenced luminescence in a MOF that may be related to exciplex formation. Stylianou *et al.* described the synthesis of a highly emissive MOF constructed from a strongly fluorescent linker ligand with an electronically isolated pyrene core [29] (see Section 3.2). For this MOF, the authors describe solid-state PL properties in which the emission is solely the result of the ligand, which is largely isolated from other ligands or possible quenching moieties. The desolvated MOF can also be resolvated using other solvents, such as H_2O, dioxane, and *p*-xylene, leading to slightly altered PL. Interestingly, while the introduction of H_2O and dioxane produce small, but expected red-shifts in λ_{max}, the introduction of *p*-xylene leads to a blue-shift (~19 nm) in λ_{max}. The authors also presented XRD data that seem to suggest that some of the *p*-xylene moieties are located in a face-to-face π–π stacking interaction with the pyrene core indicating a possible exciplex formation. However, the hypsochromic nature of the shift, together with the fact that the emission spectrum was observed to be no broader than the emission spectra of either the desolvated MOF or the MOFs resolvated with other solvents (DMF, H_2O, or dioxane), make classification of this luminescence emission as an example of exciplex formation in a MOF questionable and undetermined at this time.

5.3 Encapsulation of Lanthanide Ion Luminophores

In addition to organic molecules, it is also possible to infiltrate MOFs with metal ions to act as guest luminophores. A classic strategy for the fabrication of optically active materials is to dope a compound with luminescent lanthanide ions. Recently, this strategy was shown to be a viable option for modulating MOF luminescence. While there are numerous examples of MOFs based upon lanthanides incorporated into the framework and corresponding characterization of these materials' lanthanide-based luminescence, there are relatively few examples of MOFs infiltrated with lanthanide guests. Luo and Batten reported doping a non-lanthanide MOF with Ln^{III} cations and presented data illustrating the ability to affect the luminescence of the material [76]. In this example, a Zn^{II} MOF constructed from 1,2,4,5-benzenetetracarboxylate (H_4BTEC) generates permanent 1-periodic channels. The overall framework structure, $\{(NH_4)_2[Zn(BTEC)]\bullet 6H_2O\}_n$, is anionic and the channels are filled with counter-balancing $(NH_4)^+$ cations. Subjecting the MOF

to solutions of Tb^{III} ($Tb(ClO_4)_3$; 10^{-3} – 10^{-6} mol·L^{-1}) or Eu^{III} ($EuCl_3$;10^{-3} – 10^{-7} mol·L^{-1}) results in simple cation exchange. The authors demonstrate that the luminescence of the MOF can be tuned, based upon the choice of Ln^{III} dopant utilized. The as-synthesized MOF exhibits blue luminescence characterized as LMCT since the ligand itself was shown to be non-luminescent. Upon infiltration with dopants, the blue emission is no longer observed, however strong emission characteristic of the Ln^{III} ions is generated. Additionally, it was demonstrated that the extent of infiltration plays a role in the intensity of the emission. The MOF hybrids obtained by infusing with a higher concentration of Eu^{III} are 30 times more intense than those obtained from the lower concentration. In the case of Tb^{III} the observed intensity difference is only 8 times more in the case of higher concentration.

In a separate report, Thirumurugan and Cheetham describe a series of MOFs constructed with bismuth (Bi^{III}) in which they introduce Ln^{III} ions to modulate the luminescence of the compounds [77]. Owing to similar charge and ionic radii, bismuth containing compounds are known to behave as good hosts for Ln^{III} ions, and this knowledge has been useful for the development of doped optical materials. Upon subjecting the MOFs to solutions of Eu^{III} and Tb^{III}, the infiltrated materials (~ 2 mol% Ln^{III}) exhibit PL unique from that of the pristine as-synthesized MOF. The neat MOF material has a broad emission centered at ~420 nm that was characterized as ligand-centered $\pi^* \rightarrow n$ or $\pi^* \rightarrow \pi$ emission. After doping with the Ln^{III} ions, the emission spectra for the hybrid material exhibit characteristic peaks for Eu^{III} ($^5D_0 \rightarrow {}^7F_J$) and Tb^{III} ($^5D_4 \rightarrow {}^7F_J$), while the main ligand-centered emission is almost completely suppressed, resulting in red and green luminescence, respectively. Additionally, the authors report co-doping the MOFs, using a combination of both Eu^{III} and Tb^{III} (~2 mol% each), which results in an overall orange-colored emission and clearly demonstrates the extent to which the luminescence of these materials can be fine-tuned.

Another example, demonstrating the effect that encapsulating lanthanide-ion luminophores within a MOF has on the PL, was reported by Wang *et al.* [78]. These authors prepared a lanthanide-based MOF capable of encapsulating hydrated Ln^{III} cations by using a bent 1,2,4-trizole bridged ligand. The encapsulated cations are confined within small volumes as they are hydrogen bonded to the framework, reducing vibrational movements originating from strong O–H oscillators. These vibrational movements normally lead to quenching of the *f-f* luminescence, but their reduced contribution in these materials leads to enhanced luminescence intensity , converting the practically non-luminescent $[Ln(H_2O)_8]^{3+}$ into a strongly emissive species.

6 Applications of Luminescent MOFs

6.1 Chemical Sensors

Efficient, portable sensors are increasingly required to support the development of technologies for many fields, from medicine to homeland security, and the number of reports regarding the use of MOFs for such purposes is steadily growing. The ability to tune the emissive properties of MOFs *via* alteration of the ligand and/or metal cluster type, along with the potential for high porosity with *accessible*, uniform pores, makes MOFs inherently multifunctional materials. In addition, the precise chemical functionality and size of the pores may be selectively tailored, allowing for specific sensing and separation capabilities. These features set MOFs apart from conventional porous materials such as porous silicas and zeolites, which offer only limited degrees of synthetic tunability. As the synthetic strategies for preparing “designer” MOFs improves, so does the ability to create MOFs with functional pores. A recent review by Chen *et*

al. summarizes developments in MOF materials for molecular recognition and sensing, including MOFs that can act as molecular sieves and effectively separate gases [79]. Jiang *et al.* demonstrated that MOFs can be utilized as a stationary phase for liquid chromatography [40]. Additionally, the use of post-synthetic methodologies to alter MOF structure is of recent interest in this context [28,80-84].

As was discussed in previous sections, the emission properties of solid-state materials are often highly dependent upon details of their structure, which can potentially be tailored *via* careful selection of starting materials and growth conditions. Altering emission properties through "simple" changes in host–guest chemistry, such as solvent exchange, has been shown for a variety of porous structures, as discussed in Section 3. This may lead to solvatochromic-like effects (although, of course, the guest molecule does not "dissolve" the MOF) that are caused by altering the dielectric environment of the chromophore, resulting in different emission wavelengths, intensities, or both. Changing the solvent molecule does not just alter the dielectric environment, but may also lead to small structural changes, such as lattice expansion or contraction, changes in ligand orientation, or changes in ligand-ligand distance, which can lead to observable differences in luminescence *via* LLCT or excimer formation. Such spectral shifts are typically relatively small compared to cases in which changing the solvent results in inhibition of LMCT *vs.* ligand-based emission, for example. However, these early findings suggest that MOFs could be used and tailored for specific luminescent sensing capabilities [21]. Solvent incorporation may also result in major changes to the framework structure. For example, Zhu *et al.* reported a lanthanide MOF structure in which solvent incorporation or removal leads to reversible structural collapse, whereby luminescence is quenched and restored upon a dehydration–rehydration cycle [85]. A similar observation has been reported for one of the rare examples of luminescent MOFs from which emission is exclusively *d*-metal based, $[Cu_4I_4(DABCO)_2]_n$ (DABCO = 1,4-Diazabicyclo[2.2.2]octane). Two different structures were prepared in water and in acetonitrile [86], and the luminescence was found to vary depending on the solvent used. The MOF prepared in water shows temperature-dependent luminescence and emits at 556 nm, while the acetonitrile-incorporated MOF shows little temperature dependence and emits at 580 nm. These structures can be reversibly inter-converted by solvent exchange. The emission here is cluster-centered, and is a function of the Cu-Cu distance.

It should be noted that the examples in the previous paragraph were concerned with the effects of incorporated solvent on framework luminescence. There are many examples in the literature where this has been observed, and it may be considered to be an expected feature of significantly porous, luminescent structures. In the following sections a few such effects will be highlighted, but the focus is on the design and use of MOFs for targeted sensing purposes. Although luminescence is typically considered among the more sensitive and attractive for optical sensing methods, an elegant study by Hupp and co-workers demonstrates the first use of MOFs for sensing *via* changes in refractive index [87]. A Fabry–Pérot device fabricated from thin films of ZIF-8 (a zeolitic imidazolate framework) is found to be sensitive to various chemical vapors and gases, with analyte detection readily achievable through transmission UV-visible measurements.

6.1.1 Small Molecule and Ion Sensors

Sensing of metal ions and small molecules by emission can occur by a variety of mechanisms. Ion exchange has been used to alter sensitization in several lanthanide MOFs. Chen and co-workers report a Tb(1,3,5-BTC) structure in which anionic guests solvated in methanol were

incorporated, yielding anion-filled pores [88]. The luminescence from Tb^{III} was found to be enhanced, particularly in the presence of fluoride anion. This enhancement was attributed to a stronger hydrogen-bonding interaction between F^- and methanol leading to attenuation of the O-H stretching vibration, with concomitant reduction of the ability of this vibration to quench the sensitizing BTC ligand. Lu and co-workers demonstrated a MOF that displays sensitivity to cation exchange [89]. Here, a Tb^{III}-based MOF exhibited a significant increase in emission intensity upon exchange of K^+ with Ca^{2+}. This was ascribed to rigidification of the imidazole-4,5-dicarboxylate ligand upon complexation with Ca^{2+}, which leads to more efficient energy transfer to the lanthanide ion. Wong *et al.* reported a Tb(mucicate) structure, wherein the flexible multidentate ligand is used to differentiate between several anions, with fluorescence enhancement in the case of CO_3^{2-} and CN^- [90]. Lewis basic pyridyl sites within a luminescent porous Eu(pyridine-3,5-dicarboxylate) MOF were utilized for sensing of Cu^{II} ion [91]. This material shows significant quenching upon binding to Cu^{II}. Finally, luminescent intensity modulation was also shown for two Eu^{III}-1,4,8,11-tetraazacyclotetradecane-1,4,8,11-tetrapropionate-based MOFs, whereby Ag^I exchange significantly alters the relative transition intensities of the emissive Eu^{III} center [92].

Ion-sensing is also possible using transition metal-based frameworks, typically through alteration of LMCT efficiency. For example, a net-type anionic MOF, $\{(NH_4)_2$[Zn(1,2,4,5-benzenetetracarboxylate)]$\bullet 6H_2O\}_n$, exhibits broad luminescence centered at 440 nm, as a likely result of LMCT and/or ligand-based luminescence [93]. The open structure allows for exchange between the ammonium groups and aqueous metal cations. Titration with increasing amounts of Cu^{II} leads to quenching as a result of ion exchange, and this effect was shown for a variety of other cations in addition. Upon ion-exchange with Ln^{III} ions [76], LMCT character was no longer observed, replaced by emission typical of the lanthanide ion instead. These lanthanide-incorporated structures were subsequently doped with MCl_x solutions (M = Na^+, K^+, Zn^{2+}, Ni^{2+}, Mn^{2+}, Co^{2+}, Cu^{2+}), and significant quenching was seen for Co^{II} and Cu^{II} ions.

MOFs may be prepared in which the metal center remains unsaturated, which leads to accessible, potentially luminescent open metal sites for the sensing of small molecules. The degree of saturation of lanthanide ions in MOFs can often be manipulated via ligand exchange. For example, a porous Eu(1,3,5-BTC) MOF with open metal coordination sites shows sensitivity to a variety of solvent molecules, particularly a marked decrease in emission intensity upon exposure to acetone and an increase with DMF exchange [94]. Exchange of coordinated solvents has been shown to alter emission properties in other lanthanide-based MOFs as well. A Eu^{III} MOF with 4,4□-(hexafluoroisopropylidene)-bis(benzoic acid) linkers has been used to sense ethanol in air [95]. The Eu^{III} emission at 619 nm was monitored upon exposure, leading to a rapid decrease in luminescence intensity, which is recovered upon exposure to air. The initial quenching was attributed to an effect of the O-H stretching vibration upon coordination of ethanol to the Eu^{III} ions. Harbuzaru *et al.* also demonstrated similar use of a Eu^{III} MOF containing 1,10-phenanthroline-2,9-dicarboxylic acid linker for pH sensing applications in the biologically suitable range of pH = 5–7.5 [96].

Interruption of LMCT and MLCT processes by small molecules can lead to striking differences in luminescence properties. Jiang, *et al.* prepared Cd^{II} MOFs with the same building blocks, but with differing porosity and ligand-ligand separation [40,97]. Through alteration of the solvent volume and/or temperature, the framework porosity and LMCT signal strength was found to vary reversibly. Kobayashi *et al.* prepared a Pt/Zn-containing 5,5'-dicarboxy-2,2'-bipyridine-based MOF, which exhibits thermochromism and reversible sensitivity to solvent

vapors [98]. The thermochromic-effect is a result of dehydration of the Pt^{II} centers and the resultant change in Pt-Pt distance, which in turn affects the triplet-sensitized MLCT process. The authors also note solvatochromic effects with a mechanism similar to this thermochromic effect, whereby various solvents alter the intermetallic Pt distance.

Manipulation of ligand-based luminescence in MOFs has been shown in a variety of cases. As described in Section 3.2, Rosseinsky and co-workers prepared $[In_2(OH)_2(TBAPy)]_n$, which displays a red-shifted emission spectrum upon desolvation as a result of a reduced intermolecular ligand-ligand distance [29]. However, the spectral position and intensity nearly recover fully within 3 hours upon re-exposure to DMF. The intermolecular coupling between ligands is highly distance-dependent at short range, and addition of various guests leads to alteration in the position and intensity of the pyrene fluorescence. The authors were able to directly correlate fluorescence changes with structural changes, and note that the long lifetime and quantum yield of 6.7% make these MOFs comparable to commercial lanthanide sensors. As an additional recent example, $\{[Zn_3(1,3,5\text{-}BTC)_2]\bullet 12H_2O\}_n$ frameworks were found to be selective for ethylamine over butylamine and propylamine, exhibiting significant emission quenching of BTC-based luminescence upon increasing doses of ethylamine [99].

6.1.2 Oxygen Sensors

Phosphorescent MOFs functionalized with Ir^{III}-containing ligands have been synthesized as potential oxygen sensors [100]. A variety of Zn MOFs were prepared, wherein the ligands were Ir(2-phenylpyridine)$_3$ derivatives (see Figure 8). Structures **2** and **3** were nonporous; however structure **1** exhibits permanent porosity and reversible host-guest chemistry. Triplet-sensitized MLCT was observed from the the Ir(2-phenylpyridine)$_3$ derivatives, at 538 nm for **1** and **3**, and at 565 nm for **2**. It is well known that dioxygen rapidly quenches triplet excited states and, as expected, a decrease in the emission intensity was observed for all three structures in the presence of O_2. Interestingly, upon exposure to O_2, only the porous structure was found to respond rapidly and reversibly. A linear Stern–Volmer plot (refer to Section 2.2; eq. 5) was extracted for exposure of this porous MOF to O_2, and the luminescence quenching was shown to be reversible across multiple cycles. The nonporous MOFs have limited accessibility to the interior Ir moieties, and it also is more difficult to remove the O_2 molecules from these structures. Nonetheless, **2** and **3** were also observed to display a degree of reversibility on longer timescales than **1**.

Figure 8.

6.1.3 Detection of Explosives

Explosive detection is a topic of significant contemporary relevance, and substantial work has been carried out in this area. Efficient, inexpensive detection of DNT (a volatile indicator of TNT) and 2,3-dimethyl-2,3-dinitrobutane, (DMNB, an ingredient in plastic explosives), are of high interest in this regard. Typically, luminescent changes upon a redox reaction are used in current detection methods, although this is much more difficult to achieve for DMNB: The first example of a MOF that posses the ability to detect both markers has been reported recently [101]. The structure $[Zn_2(bpdc)_2(bpee)]_n$, (bpdc = 4,4□-biphenyldicarboxylate, bpee = 1,2-bipyridylethene) was shown to quickly (on the order of 10 seconds), reversibly, and efficiently absorb both molecules of interest, with their uptake detected through changes in the emission

properties of the MOF. Thin layers of the MOFs were exposed to vapors of DMNB and DNT, upon which red-shifted, quenched emission was rapidly observed, as shown in Figure 9. Both analytes contain nitro groups, which are known quenchers of emission. The structure maintains a 3-periodic, porous geometry in which the ligands are held at appropriate distances to minimize π–π intermolecular interactions between the ligands, and is highly emissive. It is likely that the emission is ligand-based in this MOF. DMF guests incorporated during the synthesis can be removed reversibly, although the structure is slightly distorted upon removal.

Figure 9.

6.2 Radiation Detection

Radiation detection goes hand-in-hand with the aforementioned interest in explosives detection for homeland security applications. In addition, medical devices and methods in biotechnology rely on radio-labeling. Portable, low-cost neutron detectors are currently scarce, and are often not as sensitive as required. Interestingly, the same small conjugated molecules that make for suitable ligands in MOFs can also exhibit useful scintillating properties, in particular 4,4'-stilbene dicarboxylic acid. Such molecules are known for their ability to effectively emit light upon exposure to various forms of radiation, yet their solid-state structure remains a challenge for the development of reliable, reproducible sensor devices. The structures of both 2-periodic network and 3-periodic cubic Zn stilbene MOFs (see Figure 2) provide rigid environments for the stilbene ligands, but the relative spacing and orientation differs, leading to differences in emission wavelengths and lifetimes. The 2-periodic network is denser in comparison to the porous 3-periodic cubic structure. Exposure of both MOFs to high-energy (3 MeV) protons and alpha particles leads to radioluminescence, although the materials have different Stokes shifts (Figure 10) [102]. The 3-periodic stilbene MOF has a larger Stokes shift, likely another consequence of the differences in stilbene-stilbene orientation between the two structures. It was found that these MOFs have scintillation quantum yields that are comparable to commercial scintillators. Moreover, the stability to repeated exposure outperforms anthracene, with luminescence degrading only very slowly with integrated doses up 10 MGy (1Gy = 1J/kg). The versatility of MOF syntheses and the commonality between scintillating organic groups and potential as MOF ligands leaves this area of study wide open for development.

Figure 10.

6.3 Solid-State Lighting

The tunable nature of MOFs and the ability to incorporate multiple luminophores, including guest molecules, ligands, metals, and the various potential interactions between these groups, can allow for fine-scale adjustment of the emission intensity and color of hybrid MOF materials. Solid-state lighting devices, such as OLEDs, represent highly attractive, energy-efficient methods for generation of light and are the subject of much contemporary research. In particular, white light sources for ambient lighting represent particularly interesting targets [103]. In addition to the tunability of MOF structures and emissive properties discussed previously, their high thermal stability and often intense luminescence are desirable in this context. Current white light-emitting materials typically consist of mixtures of blue and yellow emitting materials [104]. Two cases of near white light-emitting MOFs have been reported to date. Ca and Sr frameworks containing 9-fluorenone-2,7-dicarboxylic acid exhibit broad, ligand-based emission that is

dependent on the identity of the cation [105]. The rigidification of the ligand both by inclusion in the framework and by cooling to -196 °C leads to an enhancement in quantum yield. The broad emission of the pure ligand is yellow, whereas the Ca structure emits green (λ_{max} = 503 nm) and the cation exchanged Sr structure emits orange light (λ_{max} = 526 nm). Both frameworks can be excited between 380 and 460 nm, and the FWHM of the broad emission spectra are 90 nm, comparable to Ce^{III}:YAG phosphors.

The first example of a MOF material in which variable emission processes are harnessed for the purpose of generating white light was recently reported [106]. A multi-process emission profile, highly sensitive to excitation wavelength, is used to manipulate the emission color of the MOF. Wang *et al.* synthesized an Ag^{I}(4-cyanobenzoate)-based MOF that exhibits variable emission; the color is tunable from yellow to white *via* variation in excitation wavelength. The solid-state emission spectrum shows a multitude of peaks, with intensities that vary upon excitation wavelength modulation. The maximum emission is at λ = 427 nm when excited by 355 nm light, but shifts to λ = 566 nm upon excitation by 330 nm light. Excitation of the MOF at 350 nm yields a white light-emitting material (to the eye) as, at this excitation wavelength, the 427 and 566 nm bands are of nearly equal intensity. There are several physical causes for the observed emission peaks, as MLCT and ligand-based emission coexist in this structure.

6.4 Non-Linear Optics

Nonlinear optical properties (including second- and third-order processes) of both organic and inorganic materials are of great interest for a variety of purposes, such as communications, lighting, lasing, and frequency modulation. Second harmonic generation (SHG) is a nonlinear conversion of two photons of a particular frequency to a single photon with twice this frequency (*i.e.* frequency doubling). A requirement for SHG is non-centrosymmetry, which is challenging in bulk material. Donor-acceptor substituted molecules (*i.e.* push-pull conjugated) are often used. Current techniques involve assembly at liquid–air surfaces or electric field poling [107-108]. As MOFs can be tailorable in function and shape, they offer potential as scaffolds amenable to the arrangement of ligands in a non-centrosymmetric manner. Several examples of MOFs exhibiting SHG are known, including Pb^{II} complexes prepared by Yang *et al.,* for which the emission can be assigned to a metal-centered transition involving the *s*- and *p*-orbitals of the metal, sensitized by the organic ligands, a relatively rare case of main-group MLCT [41]. A porous, Cd^{II} oxalate-based MOF ionic cluster exhibited amongst the highest SHG signal recorded for MOF materials, and this structure is also sensitive to cation-exchange, illustrating the first NLO MOF with sensing potential [109]. A variety of other examples of engineered, asymmetric MOF crystals that exhibit high SHG responses have been reported [110-114]. In addition, Guo *et al.* prepared a multifunctional ferroelectric, NLO-active MOF [115].

Enhancement of standard one-photon fluorescence often leads to a concomitant increase in two-photon fluorescence, a third-order process. Although this has yet to be measured in a MOF material, the outcome may be of technological interest and warrants investigation. It has been well-documented that centrosymmetric π-conjugated molecules with quadrupolar or higher degrees of charge separation have among the highest two-photon cross-sections (δ) [116]. These often have a donor-π-donor or acceptor-π-acceptor geometry and variations thereof. Such molecules are again well-suited for MOF chemistry and many such MOF ligands are currently known or may be synthesized by straightforward protocols. In addition, coordination to the metal centers will likely improve the electron withdrawing capability of the terminal carboxylate groups, and potentially improve the two-photon fluorescence signal strength.

6.5 Bar Code Labeling

Barcoding is a method that requires reproducible, consistent materials for which read-out is rapid. White *et al.* utilized the synthetic flexibility available in MOF syntheses to introduce multiple metal centers, each of which differs in luminescence color [117]. A mixture of lanthanide ions was used to develop MOFs with differing spectral outputs, which required excitation at a single wavelength as they are all sensitized by the same organic ligand. This allows for "encoding" of the spectral profile, as lanthanide emission is typically sharp, well-resolved, and well-separated (Fig. 11). By tuning the ratio of a mixture of Ln^{III} ions (Yb, Er, Nd), a specific "code" results. The authors note the reproducibility and large diversity of codes possible. Upon coating in an adhesive matrix, the spectral profile was maintained, demonstrating the versatility of incorporation into other practical morphologies and composites.

Figure 11.

7 Conclusion

What is so unique about MOFs, aside from the spectacular pore volumes and surface areas they can exhibit, is that they possess the high local and long-range order characteristic of crystals, the synthetic versatility of organic polymers, the geometric predictability inherent in coordination bonding, *and* often stable nanoporosity. This amazing combination of properties is only beginning to be explored and is likely to lead to many surprises as scientists in fields beyond chemistry consider MOFs from their own perspectives and with their own specialized expertise. The examples cited in this chapter demonstrate that luminescent MOFs are not only a rapidly expanding subset with tremendous potential for a wide variety of applications, but are also an exciting venue for building new, fundamental understanding of electronic structure, energy transfer, and light emission. It therefore seems likely that research to date represents only the beginning of a long and interesting scientific story.

Acknowledgements

This research was funded by the Defense Threat Reduction Agency under contract 074325I-0, the US Dept. of Energy Office of Proliferation Detection Programs, and the Sandia Laboratory Directed Research and Development Program. Sandia National Laboratories is a multi-program laboratory managed and operated by Sandia Corporation, a wholly owned subsidiary of Lockheed Martin Corporation, for the U.S. Department of Energy's National Nuclear Security Administration under contract DE-AC04-94AL85000. CAB acknowledges support from NSF Discovery Corps Fellowship Grant CHE0725176.

8 References

1. Allendorf, M.D., Bauer, C.A., Bhakta, R.K. and Houk, R.J.T. (2009) Luminescent metal-organic frameworks. *Chem. Soc. Rev.,* **38**(5), 1330-1352.

2. McCapra, F. (1966) Chemiluminescence of Organic Compounds. *Quarter. Rev.,* **20**(4), 485-510.
3. Dodeigne, C., Thunus, L. and Lejeune, R. (2000) Chemiluminescence as a diagnostic tool. A review. *Talanta,* **51**(3), 415-439.
4. Aslan, K. and Geddes, C.D. (2009) Metal-enhanced chemiluminescence: advanced chemiluminescence concepts for the 21st century. *Chem. Soc. Rev.,* **38**(9), 2556-2564.
5. Widder, E.A. (2010) Bioluminescence in the Ocean: Origins of Biological, Chemical, and Ecological Diversity. *Science,* **328**(5979), 704-708.
6. Tsien, R.Y. (1998) The green fluorescent protein. *Annu. Rev. Biochem.,* **67**(1), 509-544.
7. Meighen, E.A. (1991) Molecular-Biology of Bacterial Bioluminescence. *Microbiol. Rev.,* **55**(1), 123-142.
8. Mitschke, U. and Bauerle, P. (2000) The electroluminescence of organic materials. *J. Mater. Chem.,* **10**(7), 1471-1507.
9. Miao, W.J. (2008) Electrogenerated chemiluminescence and its biorelated applications. *Chem. Rev.,* **108**(7), 2506-2553.
10. Sweeting, L.M. (2001) Triboluminescence with and without Air. *Chem. Mater.,* **13**(3), 854-870.
11. Chandra, B.P. and Rathore, A.S. (1995) Classification of Mechanoluminescence. *Cryst. Res. Technol.,* **30**(7), 885-896.
12. Chandra, B.P. (1981) Mechanoluminescence and Piezoelectric Behavior of Molecular-Crystals. *Phys. Status Solidi A,* **64**(1), 395-405.
13. Schulman, S.G. (1985) Luminescence Spectroscopy: An Overview, in *Molecular Luminescence Spectroscopy - Methods and Applications: Part 1*, (ed Schulman, S. G.), John Wiley & Sons, New York, pp. 1-28.
14. Vogler, A. and Kunkely, H. (2001) Luminescence in Metal Complexes: Diversity of excited states, in *Transition Metal and Rare Earth Compounds*, (ed Yersin, H.), Springer, Berlin, pp. 183-184.
15. Ronda, C. (ed) (2008) *Luminescence: From Theory to Applications*, Wiley, Weinheim.
16. Birks, J.B. (1970) *Photophysics of Aromatic Molecules*, Wiley-Interscience, London.
17. Valeur, B. and Brochon, J.-C. (ed) (2001) *New trends in fluorescence spectroscopy : applications to chemical and life science*, Springer, New York.
18. Lakowicz, J.R. (2006) *Principles of fluorescence spectroscopy*, Springer, New York.
19. Balzani, V., Bergamini, G., Campagna, S. and Puntoriero, F. (2007) Photochemistry and Photophysics of Coordination Compounds : Overview and General Concepts, in *Photochemistry and Photophysics of Coordination Compounds I*, (ed Balzani, V.and Campagna, S.), Springer, Berlin, pp. 1-36.
20. Eddaoudi, M., Kim, J., Rosi, N., Vodak, D., Wachter, J., O'Keeffe, M. and Yaghi, O.M. (2002) Systematic design of pore size and functionality in isoreticular MOFs and their application in methane storage. *Science,* **295**(5554), 469-472.
21. Bauer, C., Timofeeva, T., Settersten, T., Patterson, B., Liu, V., Simmons, B. and Allendorf, M. (2007) Influence of connectivity and porosity on ligand-based luminescence in zinc metal-organic frameworks. *J. Am. Chem. Soc.,* **129**(22), 7136-7144.
22. Meek, S.T., Houk, R.J.T., Doty, F.P. and Allendorf, M.D. (2010) Luminescent Metal-Organic Frameworks: A Nanolaboratory for Probing Energy Transfer via Interchromophore Interactions. *ECS Transactions,* **28**(3), 137-143.

23. Bordiga, S., Lamberti, C., Ricchiardi, G., Regli, L., Bonino, F., Damin, A., Lillerud, K.-P., Bjorgenb, M. and Zecchina, A. (2004) Electronic and vibrational properties of a MOF-5 metal–organic framework: ZnO quantum dot behaviour. *Chem. Commun.,* (20), 2300-2301.
24. Civalleri, B., Napoli, F., Noel, Y., Roetti, C. and Dovesi, R. (2006) Ab-initio prediction of materials properties with CRYSTAL: MOF-5 as a case study. *CrystEngComm,* **8**(5), 364-371.
25. Feng, P.L., Perry IV, J.J., Nikodemski, S., Meek, S.T. and Allendorf, M.D. (2010) Assessing the Purity of Metal-Organic Frameworks Using Photoluminescence: MOF-5, ZnO Quantum Dots, and Framework Decomposition. *J. Am. Chem. Soc.,* (Submitted).
26. Saltiel, J. (1967) Perdeuteriostilbene. Role of Phantom States in *cis-trans* Photoisomerization of Stilbenes. *J. Am. Chem. Soc.,* **89**(4), 1036-1037.
27. Waldeck, D.H. (1991) Photoisomerization Dynamics of Stilbenes. *Chem. Rev.,* **91**(3), 415-436.
28. Jones, S. and Bauer, C. (2009) Diastereoselective Heterogeneous Bromination of Stilbene in a Porous Metal-Organic Framework. *J. Am. Chem. Soc.,* **131**(35), 12516-12517.
29. Stylianou, K.C., Heck, R., Chong, S.Y., Bacsa, J., Jones, J.T.A., Khimyak, Y.Z., Bradshaw, D. and Rosseinsky, M.J. (2010) A Guest-Responsive Fluorescent 3D Microporous Metal-Organic Framework Derived from a Long-Lifetime Pyrene Core. *J. Am. Chem. Soc.,* **132**(12), 4119-4130.
30. Huh, S., Jung, S., Kim, Y., Kim, S. and Park, S. (2010) Two-dimensional metal-organic frameworks with blue luminescence. *Dalton Trans.,* **39**(5), 1261-1265.
31. Lu, Z., Wen, L., Ni, Z., Li, Y., Zhu, H. and Meng, Q. (2007) Syntheses, Structures, and Photoluminescent and Magnetic Studies of Metal-Organic Frameworks Assembled with 5-Sulfosalicylic acid and 1,4-Box(imidazol-1-ylmethyl)-benzene. *Cryst. Growth Des.,* **7**(2), 268-274.
32. Park, B., Eom, G., Kim, S., Kwak, H., Yoo, S., Lee, Y., Kim, C., Kim, S. and Kim, Y. (2010) Construction of Cd(II) compounds with a chelating ligand 2,2 '-dipyridiylamine (Hdpa): Anion effect, catalytic activities and luminescence. *Polyhedron,* **29**(2), 773-786.
33. Zou, R., Abdel-Fattah, A., Xu, H., Burrell, A., Larson, T., McCleskey, T., Wei, Q., Janicke, M., Hickmott, D., Timofeeva, T. and Zhao, Y. (2010) Porous Metal-Organic Frameworks Containing Alkali-Bridged Two-Fold Interpenetration: Synthesis, Gas Adsorption, and Fluorescence Properties. *Cryst. Growth Des.,* **10**(3), 1301-1306.
34. Chen, W., Wang, J.-Y., Chen, C., Yuan, Q.Y.-M., Chen, J.-S. and Wang, S.-N. (2003) Photoluminescent Metal−Organic Polymer Constructed from Trimetallic Clusters and Mixed Carboxylates. *Inorg. Chem.,* **42**(4), 944−946.
35. Dai, J.-C., Wu, X.-T., Fu, Z.-Y., Cui, C.-P., Hu, S.-M., Du, W.-X., Wu, L.-M., Zhang, H.-H. and Sun, R.-Q. (2002) Synthesis, Structure, and Fluorescence of the Novel Cadmium(II)−Trimesate Coordination Polymers with Different Coordination Architectures. *Inorg. Chem.,* **41**(6), 1391-1396.
36. Dai, J.-C., Wu, X.-T., Fu, Z.-Y., Hu, S.-M., Du, W.-X., Cui, C.-P., Wu, L.-M., Zhang, H.-H. and Sun, R.-Q. (2002) A novel ribbon-candy-like supramolecular architecture of cadmium(II)–terephthalate polymer with giant rhombic channels: twofold interpenetration of the 3D $8^2$10-a net *Chem. Commun.,* (1), 12-13.
37. Fang, Q., Zhu, G., Xin Shi, G.W., Ge Tian, R.W. and Qiu, S. (2004) Synthesis, structure and fluorescence of a novel three-dimensional inorganic–organic hybrid polymer

constructed from trimetallic clusters and mixed carboxylate ligands *J. Solid State Chem.,* **177**(4-5), 1060-1066
38. Huang, Y.-Q., Ding, B., Song, H.-B., Zhao, B., Ren, P., Cheng, P., Wang, H.-G., Liao, D.-Z. and Yan, S.-P. (2006) A novel 3D porous metal–organic framework based on trinuclear cadmium clusters as a promising luminescent material exhibiting tunable emissions between UV and visible wavelengths. *Chem. Commun.,* (47), 4906-4908.
39. Zeng, F., Ni, J., Wang, Q., Ding, Y., Ng, S., Zhu, W. and Xie, Y. (2010) Synthesis, Structures, and Photoluminescence of Zinc(II), Cadmium(II), and Mercury(II) Coordination Polymers Constructed from Two Novel Tetrapyridyl Ligands. *Cryst. Growth Des.,* **10**(4), 1611-1622.
40. Jiang, H., Tatsu, Y., Lu, Z. and Xu, Q. (2010) Non-, Micro-, and Mesoporous Metal-Organic Framework Isomers: Reversible Transformation, Fluorescence Sensing, and Large Molecule Separation. *J. Am. Chem. Soc.,* **132**(16), 5586-5587.
41. Yang, E.-C., Li, J., Ding, B., Liang, Q.-Q., Wang, X.-G. and Zhao, X.-J. (2008) An eight-connected 3D lead(II) metal-organic framework with octanuclear lead(II) as a secondary building unit: synthesis, characterization and luminescent property. *CrystEngComm,* **10**(2), 158-161.
42. He, X., Lu, C.Z., Wu, C.D. and Chen, L.J. (2006) A series of one- to three-dimensional copper coordination polymers based on N-heterocyclic ligands. *Eur. J. Inorg. Chem.,* **2006**(12), 2491-2503.
43. Zhang, S., Wang, Z., Zhang, H.H., Cao, Y.N., Sun, Y.X., Chen, Y.P., Huang, C.C. and Yu, X.H. (2007) Self-assembly of two fluorescent supramolecular frameworks constructed from unsymmetrical benzene tricarboxylate and bipyridine. *Inorg. Chim. Acta,* **360**(8), 2704-2710.
44. Han, L., Yuan, D.Q., Wu, B.L., Liu, C.P. and Hong, M.L. (2206) Syntheses, structures and properties of three novel coordination polymers with a flexible asymmetric bridging ligand. *Inorg. Chim. Acta,* **359**(7), 2232-2240.
45. Eliseeva, S.V. and Bunzli, J.C.G. (2010) Lanthanide luminescence for functional materials and bio-sciences. *Chem. Soc. Rev.,* **39**(1), 189-227.
46. Binnemans, K. (2009) Lanthanide-Based Luminescent Hybrid Materials. *Chem. Rev.,* **109**(9), 4283-4374.
47. Sabbatini, N., Guardigli, M. and Lehn, J.M. (1993) Luminescent Lanthanide Complexes as Photochemical Supramolecular Devices. *Coord. Chem. Rev.,* **123**(1-2), 201-228.
48. Chandler, B.D., Yu, J.O., Cramb, D.T. and Shimizu, G.K.H. (2007) Series of lanthanide-alkali metal-organic frameworks exhibiting luminescence and permanent microporosity. *Chem. Mater.,* **19**(18), 4467-4473.
49. Gandara, F., Garcia-Cortes, A., Cascales, C., Gomez-Lor, B., Gutierrez-Puebla, E., Iglesias, M., Monge, A. and Snejko, N. (2007) Rare earth arenedisulfonate metal-organic frameworks: An approach toward polyhedral diversity and variety of functional compounds. *Inorg. Chem.,* **46**(9), 3475-3484.
50. Huang, Y., Yan, B., Shao, M. and Chen, Z.X. (2007) A new family of dimeric lanthanide(III) complexes: Synthesis, structures and photophysical property. *J. Mol. Struct.,* **871**(1-3), 59-66.
51. Huang, Y.G., Wu, B.L., Yuan, D.Q., Xu, Y.Q., Jiang, F.L. and Hong, M.C. (2007) New lanthanide hybrid as clustered infinite nanotunnel with 3D Ln-O-Ln framework and (3,4)-connected net. *Inorg. Chem.,* **46**(4), 1171-1176.

52. Mahata, P. and Natarajan, S. (2007) A New Series of Three-Dimensional Metal−Organic Framework, $[M_2(H_2O)][C_5NH_3(COO)_2]_3 \cdot 2H_2O$, M = La, Pr, and Nd: Synthesis, Structure, and Properties. *Inorg. Chem.,* **46**(4), 1250-1258.
53. Mahata, P., Ramya, K.V. and Natarajan, S. (2007) Synthesis, structure and optical properties of rare-earth benzene carboxylates. *Dalton Trans.,* **36**(36), 4017-4026.
54. Song, X.-Q., Liu, W.S., Dou, W., Wang, Y.W., Zheng, J.R. and Zang, Z.P. (2008) Structure Variation and Luminescence Properties of Lanthanide Complexes Incorporating a Naphthalene-Derived Chromophore Featuring Salicylamide Pendant Arms. *Eur. J. Inorg. Chem.,* **2008**(11), 1901-1912.
55. Sonnauer, A., Nather, C., Hoppe, H.A., Senker, J. and Stock, N. (2007) Systematic investigation of lanthanide phosphonatoethanesulfonate framework structures by high-throughput methods, $Ln(O_3P\text{-}C_2H_4\text{-}SO_3)(H_2O)$ (Ln = La-Dy). *Inorg. Chem.,* **46**(23), 9968-9974.
56. Sun, Y.Q. and Yang, G.Y. (2007) Organic-inorganic hybrid materials constructed from inorganic lanthanide sulfate skeletons and organic 4,5-imidazoledicarboxylic acid. *Dalton Trans.,* **36**(34), 3771-3781.
57. van der Horst, M.G., van Albada, G.A., Ion, R.M., Mutikainen, I., Turpeinen, U., Tanase, S. and Reedijk, J. (2008) Extended Networks Generated from the Interaction of Rare-Earth (III) Ions and Pyridine-2-carboxamide-Based Ligands. *Eur. J. Inorg. Chem.,* **2008**(13), 2170-2176.
58. Xu, H.T. and Li, Y.D. (2004) The organic ligands as template: the synthesis, structures and properties of a series of the layered structure rare-earth coordination polymers. *J. Mol. Struct.,* **690**(1-3), 137-143.
59. Yue, Q., Yang, J., Li, G.H., Li, G.D. and Chen, J.S. (2006) Homochiral porous lanthanide phosphonates with 1D triple-strand helical chains: Synthesis, photoluminescence, and adsorption properties. *Inorg. Chem.,* **45**(11), 4431-4439.
60. Zhang, X.J., Xing, Y.H., Sun, Z., Han, J., Zhang, Y.H., Ge, M.F. and Niu, S.Y. (2007) A Series of Two-Dimensional Metal-Organic Frameworks Based on the Assembly of Rigid and Flexible Carboxylate-Containing Mixed Ligands with Lanthanide Metal Salts. *Cryst. Growth Des.,* **7**(10), 2041-2046.
61. Li, X., Sun, H.L., Wu, X.S., Qiu, X. and Du, M. (2010) Unique (3,12)-Connected Porous Lanthanide-Organic Frameworks Based on Ln(4)O(4) Clusters: Synthesis, Crystal Structures, Luminescence, and Magnetism. *Inorg. Chem.,* **49**(4), 1865-1871.
62. Choi, J.R., Tachikawa, T., Fujitsuka, M. and Majima, T. (2010) Europium-Based Metal-Organic Framework as a Photocatalyst for the One-Electron Oxidation of Organic Compounds. *Langmuir,* **26**(13), 10437-10443.
63. Lin, Z.-J., Xu, B., Liu, T.-F., Cao, M.-N., Lu, J. and Cao, R. (2010) A Series of Lanthanide Metal–Organic Frameworks Based on Biphenyl-3,4',5-tricarboxylate: Syntheses, Structures, Luminescence and Magnetic Properties. *Eur. J. Inorg. Chem.,* **2010**(24), 3842-3849.
64. Soares-Santos, P., Cunha-Silva, L., Paz, F., Ferreira, R., Rocha, J., Carlos, L. and Nogueira, H. (2010) Photo luminescent Lanthanide-Organic Bilayer Networks with 2,3-Pyrazinedicarboxylate and Oxalate. *Inorg. Chem.,* **49**(7), 3428-3440.
65. Li, X., Wu, B.L., Niu, C.Y., Niu, Y.Y. and Zhang, H.Y. (2009) Syntheses of Metal-2-(Pyridin-4-yl)-1H-imidazole-4,5-dicarboxylate Networks with Topological Diversity:

Gas Adsorption, Thermal Stability and Fluorescent Emission Properties. *Cryst. Growth Des.,* **9**(8), 3423-3431.

66. de Lill, D.T., de Bettencourt-Dias, A. and Cahill, C.L. (2007) Exploring lanthanide luminescence in metal-organic frameworks: Synthesis, structure, and guest-sensitized luminescence of a mixed europium/terbium-adipate framework and a terbium-adipate framework. *Inorg. Chem.,* **46**(10), 3960-3965.
67. Soares-Santos, P.C.R., Cunha-Silva, L., Paz, F.A.A., Ferreira, R.A.S., Rocha, J., Trindade, T., Carlos, L.D. and Nogueira, H.I.S. (2008) Photoluminescent 3D Lanthanide-Organic Frameworks with 2,5-Pyridinedicarboxylic and 1,4-Phenylenediacetic Acids. *Cryst. Growth Des.,* **8**(7), 2505-2516.
68. Richardson, F.S. (1982) Terbium(III) and Europium(III) Ions as Luminescent Probesand Stains for Biomolecular Systems. *Chem. Rev.,* **82**(5), 541-552.
69. Serre, C., Millange, F., Thouvenot, C., Gardant, N., Pellé, F. and Férey, G. (2004) Synthesis, characterisation and luminescent properties of a new three-dimensional lanthanide trimesate: M((C_6H_3)–$(CO_2)_3$) (M= Y, Ln) or MIL-78. *J. Mater. Chem.,* **14**(10), 1540-1543.
70. Muller, M., Devaux, A., Yang, C.H., De Cola, L. and Fischer, R.A. (2010) Highly emissive metal-organic framework composites by host-guest chemistry. *Photochem. Photobiol. Sci.,* **9**(6), 846-853.
71. Zhang, X., Ballem, M.A., Ahren, M., Suska, A., Bergman, P. and Uvdal, K. (2010) Nanoscale Ln(III)-Carboxylate Coordination Polymers (Ln = Gd, Eu, Yb): Temperature-Controlled Guest Encapsulation and Light Harvesting. *J. Am. Chem. Soc.,* **132**(30), 10391-10397.
72. Park, Y.K., Choi, S.B., Kim, H., Kim, K., Won, B.H., Choi, K., Choi, J.S., Ahn, W.S., Won, N., Kim, S., Jung, D.H., Choi, S.H., Kim, G.H., Cha, S.S., Jhon, Y.H., Yang, J.K. and Kim, J. (2007) Crystal structure and guest uptake of a mesoporous metal-organic framework containing cages of 3.9 and 4.7 nm in diameter. *Angew. Chem., Int. Ed.,* **46**(43), 8230-8233.
73. Cornil, J., dos Santos, D.A., Crispin, X., Silbey, R. and Bredas, J.L. (1998) Influence of interchain interactions on the absorption and luminescence of conjugated oligomers and polymers: A quantum-chemical characterization. *J. Am. Chem. Soc.,* **120**(6), 1289-1299.
74. Wagner, B.D., McManus, G.J., Moulton, B. and Zaworotko, M.J. (2002) Exciplex fluorescence of {[Zn(bipy)$_{1.5}$(NO_3)$_2$] center dot CH_3OH center dot 0.5pyrene}$_n$: a coordination polymer containing intercalated pyrene molecules (bipy = 4,4 '-bipyridine). *Chem. Commun.,* (18), 2176-2177.
75. McManus, G.J., Perry, J.J., Perry, M., Wagner, B.D. and Zaworotko, M.J. (2007) Exciplex fluorescence as a diagnostic probe of structure in coordination polymers of Zn2+ and 4,4'-bipyridine containing intercalated pyrene and enclathrated aromatic solvent guests. *J. Am. Chem. Soc.,* **129**(29), 9094-9101.
76. Luo, F. and Batten, S.R. (2010) Metal-organic framework (MOF): lanthanide(III)-doped approach for luminescence modulation and luminescent sensing. *Dalton Trans.,* **39**(19), 4485-4488.
77. Thirumurugan, A. and Cheetham, A.K. (2010) Anionic Metal–Organic Frameworks of Bismuth Benzenedicarboxylates: Synthesis, Structure and Ligand-Sensitized Photoluminescence. *Eur. J. Inorg. Chem.,* (ASAP), DOI:10.1002/ejic.201000535.

78. Wang, P., Ma, J.P. and Dong, Y.B. (2009) Guest-Driven Luminescence: Lanthanide-Based Host-Guest Systems with Bimodal Emissive Properties Based on a Guest-Driven Approach. *Chem.-Eur. J.,* **15**(40), 10432-10445.
79. Chen, B., Xiang, S. and Qian, G. (2010) Metal-organic frameworks with functional pores for recognition of small molecules. *Acc. Chem. Res.,* **43**(8), 1115-1124.
80. Cohen, S.M. (2009) Supramolecular Chemistry: Molecular crystal balls. *Nature,* **461**(7264), 602-603.
81. Ingleson, M.J., Heck, R., Gould, J.A. and Rosseinsky, M.J. (2009) Nitric Oxide Chemisorption in a Postsynthetically Modified Metal-Organic Framework. *Inorg. Chem.,* **48**(21), 9986-9988.
82. Song, Y.-F. and Cronin, L. (2008) Postsynthetic covalent modification of metal-organic framework (MOF) materials. *Angew. Chem., Int. Ed.,* **47**(25), 4635-4637.
83. Wang, Z. and Cohen, S. (2009) Postsynthetic modification of metal-organic frameworks. *Chem. Soc. Rev.,* **38**(5), 1315-1329.
84. Wang, Z., Tanabe, K. and Cohen, S. (2010) Tuning Hydrogen Sorption Properties of Metal-Organic Frameworks by Postsynthetic Covalent Modification. *Chem.-Eur. J.,* **16**(1), 212-217.
85. Zhu, W.H., Wang, Z.M. and Gao, S. (2007) Two 3D porous lanthanide-fumarate-oxalate frameworks exhibiting framework dynamics and luminescent change upon reversible de- and rehydration. *Inorg. Chem.,* **46**(4), 1337-1342.
86. Braga, D., Maini, L., Mazzeo, P. and Ventura, B. (2010) Reversible Interconversion between Luminescent Isomeric Metal-Organic Frameworks of [Cu4I4(DABCO)(2)] (DABCO=1,4-Diazabicyclo[2.2.2]octane). *Chem.-Eur. J.,* **16**(5), 1553-1559.
87. Lu, G. and Hupp, J. (2010) Metal-Organic Frameworks as Sensors: A ZIF-8 Based Fabry-Perot Device as a Selective Sensor for Chemical Vapors and Gases. *J. Am. Chem. Soc.,* **132**(23), 7832-7833.
88. Chen, B.L., Wang, L.B., Zapata, F., Qian, G.D. and Lobkovsky, E.B. (2008) A luminescent microporous metal-organic framework for the recognition and sensing of anions. *J. Am. Chem. Soc.,* **130**(21), 6718-6719.
89. Lu, W.G., Jiang, L., Feng, X.L. and Lu, T.B. (2009) Three-Dimensional Lanthanide Anionic Metal-Organic Frameworks with Tunable Luminescent Properties Induced by Cation Exchange. *Inorg. Chem.,* **48**(15), 6997-6999.
90. Wong, K.-L., Law, G.-L., Yang, Y.-Y. and Wong, W.-T. (2006) A Highly Porous Luminescent Terbium–Organic Framework for Reversible Anion Sensing. *Adv. Mater.,* **18**(8), 1051-1054.
91. Chen, B.L., Wang, L.B., Xiao, Y.Q., Fronczek, F.R., Xue, M., Cui, Y.J. and Qian, G.D. (2009) A Luminescent Metal-Organic Framework with Lewis Basic Pyridyl Sites for the Sensing of Metal Ions. *Angew. Chem., Int. Ed.,* **48**(3), 500-503.
92. Liu, W., Jiao, T., Li, Y., Liu, Q., Tan, M., Wang, H. and Wang, L. (2004) Lanthanide coordination polymers and their Ag^{+}-modulated fluorescence. *J. Am. Chem. Soc.,* **126**(8), 2280-2281.
93. Liu, S., Li, J. and Luo, F. (2010) The first transition-metal metal-organic framework showing cation exchange for highly selectively sensing of aqueous Cu(II) ions. *Inorg. Chem. Commun.,* **13**(7), 870-872.

94. Xiao, Y., Wang, L., Cui, Y., Chen, B., Zapata, F. and Qian, G. (2009) Molecular sensing with lanthanide luminescence in a 3D porous metal-organic framework. *J. Alloys Compd.,* **484**(1-2), 601-604.
95. Harbuzaru, B.V., Corma, A., Rey, F., Atienzar, P., Jorda, J.L., Garcia, H., Ananias, D., Carlos, L.D. and Rocha, J. (2008) Metal-organic nanoporous structures with anisotropic photoluminescence and magnetic properties and their use as sensors. *Angew. Chem., Int. Ed.,* **47**(6), 1080-1083.
96. Harbuzaru, B.V., Corma, A., Rey, F., Jorda, J.L., Ananias, D., Carlos, L.D. and Rocha, J. (2009) A Miniaturized Linear pH Sensor Based on a Highly Photoluminescent Self-Assembled Europium(III) Metal-Organic Framework. *Angew. Chem., Int. Ed.,* **48**(35), 6476-6479.
97. Jiang, C., Yu, Z., Jiao, C., Wang, S., Li, J., Wang, Z. and Cui, Y. (2004) Luminescent Zn and Cd coordination polymers. *Eur. J. Inorg. Chem.,* **2004**(23), 4669-4674.
98. Kobayashi, A., Hara, H., Noro, S. and Kato, M. (2010) Multifunctional sensing ability of a new Pt/Zn-based luminescent coordination polymer. *Dalton Trans.,* **39**(14), 3400-3406.
99. Qiu, L., Li, Z., Wu, Y., Wang, W., Xu, T. and Jiang, X. (2008) Facile synthesis of nanocrystals of a microporous metal-organic framework by an ultrasonic method and selective sensing of organoamines. *Chem. Commun.,* (31), 3642-3644.
100. Xie, Z.G., Ma, L.Q., deKrafft, K.E., Jin, A. and Lin, W.B. (2010) Porous Phosphorescent Coordination Polymers for Oxygen Sensing. *J. Am. Chem. Soc.,* **132**(3), 922-923.
101. Lan, A.J., Li, K.H., Wu, H.H., Olson, D.H., Emge, T.J., Ki, W., Hong, M.C. and Li, J. (2009) A Luminescent Microporous Metal-Organic Framework for the Fast and Reversible Detection of High Explosives. *Angew. Chem., Int. Ed.,* **48**(13), 2334-2338.
102. Doty, F.P., Bauer, C.A., Skulan, A.J., Grant, P.G. and Allendorf, M.D. (2009) Scintillating Metal-Organic Frameworks: A New Class of Radiation Detection Materials. *Adv. Mater.,* **21**(1), 95-101.
103. Nakamura, H. (2009) Recent Development of White LEDs and Solid State Lighting. *Light Eng.,* **17**(4), 13-17.
104. Chang, C., Chen, C., Wu, C., Chang, S., Hung, J. and Chi, Y. (2010) High-color-rendering pure-white phosphorescent organic light-emitting devices employing only two complementary colors. *Org. Electron,* **11**(2), 266-272.
105. Furman, J.D., Warner, A.Y., Teat, S.J., Mikhailovsky, A.A. and Cheetham, A.K. (2010) Tunable, Ligand-Based Emission from Inorganic-Organic Frameworks: A New Approach to Phosphors for Solid State Lighting and Other Applications. *Chem. Mater.,* **22**(7), 2255-2260.
106. Wang, M.S., Guo, S.P., Li, Y., Cai, L.Z., Zou, J.P., Xu, G., Zhou, W.W., Zheng, F.K. and Guo, G.C. (2009) A Direct White-Light-Emitting Metal-Organic Framework with Tunable Yellow-to-White Photoluminescence by Variation of Excitation Light. *J. Am. Chem. Soc.,* **131**(38), 13572-13573.
107. Prasad, P.N. and Williams, D.J. (1991) *Introduction to Nonlinear Optical Effects in Molecules and Polymers*, John Wiley, New York.
108. Nalwa, H.S. and Miyata, S. (1997) *Nonlinear Optics of Organic Molecules and Polymers*, CRC Press, Boca Raton, FL.
109. Liu, Y., Li, G., Li, X. and Cui, Y. (2007) Cation-dependent non-linear optical behavior in an octupolar 3D anionic metal-organic open framework. *Angew. Chem., Int. Ed.,* **46**(33), 6301-6304.

110. Evans, O.R. and Lin, W.B. (2002) Crystal engineering of NLO materials based on metal-organic coordination networks. *Acc. Chem. Res.,* **35**(7), 511-522.
111. Liu, G., Zhu, K., Xu, H., Nishihara, S., Huang, R. and Ren, X. (2010) Five 3D metal-organic frameworks constructed from V-shaped polycarboxylate acids and flexible imidazole-based ligands. *CrystEngComm.,* **12**(4), 1175-1185.
112. Liu, T., Lu, J., Guo, Z., Proserpio, D. and Cao, R. (2010) New Metal-Organic Framework with Uninodal 4-Connected Topology Displaying Interpenetration, Self-Catenation, and Second-Order Nonlinear Optical Response. *Cryst. Growth Des.,* **10**(4), 1489-1491.
113. Wen, L.-L., Dang, D.-B., Duan, C.-Y., Li, Y.-Z., Tian, Z.-F. and Meng, Q.-J. (2005) 1D Helix, 2D Brick-Wall and Herringbone, and 3D Interpenetration d10 Metal−Organic Framework Structures Assembled from Pyridine-2,6-dicarboxylic Acid N-Oxide. *Inorg. Chem.,* **44**(20), 7161-7170.
114. Xiong, R.-G., Zuo, J.-L., You, X.-Z., Abrahams, B.F., Bai, Z.-P., Chec, C.-M. and Fund, H.-K. (2000) Opto-electronic multifunctional chiral diamondoid-network coordination polymer: bis{4-[2-(4-pyridyl)ethenyl]benzoato}zinc with high thermal stability. *Chem. Commun.,* (20), 2061-2062.
115. Guo, Z., Cao, R., Wang, X., Li, H., Yuan, W., Wang, G., Wu, H. and Li, J. (2009) A Multifunctional 3D Ferroelectric and NLO-Active Porous Metal-Organic Framework. *J. Am. Chem. Soc.,* **131**(20), 6894-6895.
116. Albota, M., Beljonne, D., Bredas, J., Ehrlich, J., Fu, J., Heikal, A., Hess, S., Kogej, T., Levin, M., Marder, S., McCord-Maughon, D., Perry, J., Rockel, H., Rumi, M., Subramaniam, C., Webb, W., Wu, X. and Xu, C. (1998) Design of organic molecules with large two-photon absorption cross sections. *Science,* **281**(5383), 1653-1656.
117. White, K.A., Chengelis, D.A., Gogick, K.A., Stehman, J., Rosi, N.L. and Petoud, S. (2009) Near-Infrared Luminescent Lanthanide MOF Barcodes. *J. Am. Chem. Soc.,* **131**(50), 18069-18071.

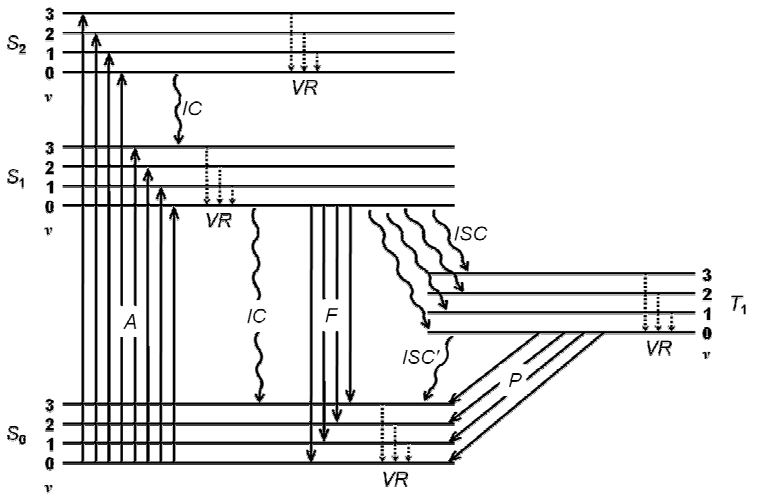

Figure 1. Jablonski diagram depicting the photophysical processes of a conjugated organic molecule. Absorption (*A*) of energy is followed by fast, non-radiative processes such as vibrational relaxation (*VR*) and internal conversion (*IC*) down to the lowest vibration level of the first excited state ($S_{1,0}$). From here there are three process for the deactivation of $S_{1,0}$; the non-radiative processes of internal conversion (*IC*) and singlet-triplet intersystem crossing (*ISC*), as well as the radiative process of fluorescence (*F*). If the deactivation process leads to singlet-triplet *ISC*, further relaxation from the lowest excited triplet state ($T_{1,0}$) can proceed through either radiative (Phosphorescence, *P*) or non-radiative (triplet-singlet intersystem crossing, *ISC'*) deactivation to the ground state.

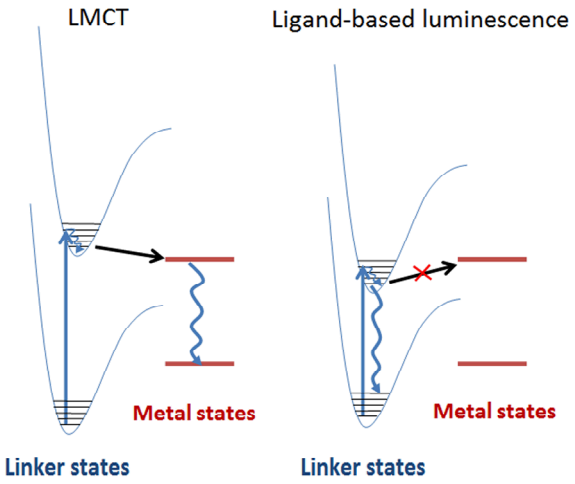

Figure 2. Energy level diagram depicting HOMO and LUMO states of the organic ligand, and intersystem crossing (LMCT) to emissive metal states (left). If π-conjugation in the ligand is increased, the HOMO-LUMO gap is decreased, making LMCT inefficient and, therefore, ligand-based emission is observed (right). In addition, coupling to surrounding solvent or guest molecules may also affect the efficiency of these transitions for porous structures.

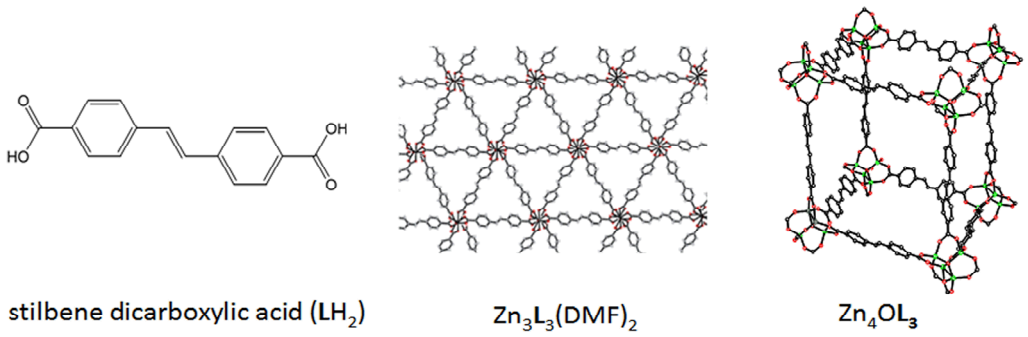

Figure 3. Structure of 4,4□-stilbene dicarboxylic acid, the layered 2D Zn stilbene MOF structure, and an individual cubic unit of the catenated 3D Zn stilbene MOF structure.

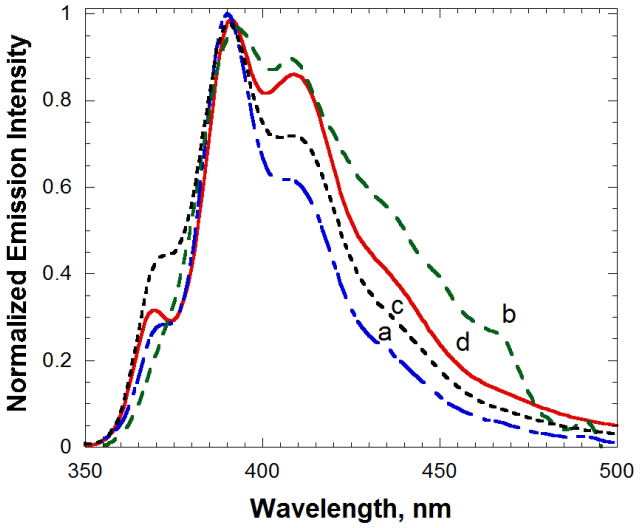

Figure 4. Emission spectra of 3D Zn stilbene MOFs with (a) chloroform guest molecules and (b) after full evacuation. The emission spectra of partially brominated Zn stilbene MOFs in (c) a chloroform environment and (d) *after full evacuation* reveal the stability of the structure to bromination and subsequent evacuation, as evidenced by their similarity to (a).

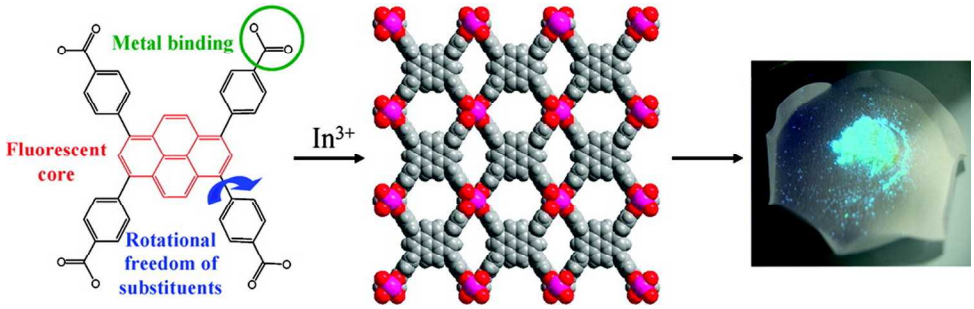

Figure 5. $[In_2(OH)_2(TBAPy)]$ MOFs exhibit bright fluorescence in the extended network. The lifetime and intensity of the emission increases due to strong coordination within the framework structure. Reprinted with permission from [28]. Copyright 2010 American Chemical Society.

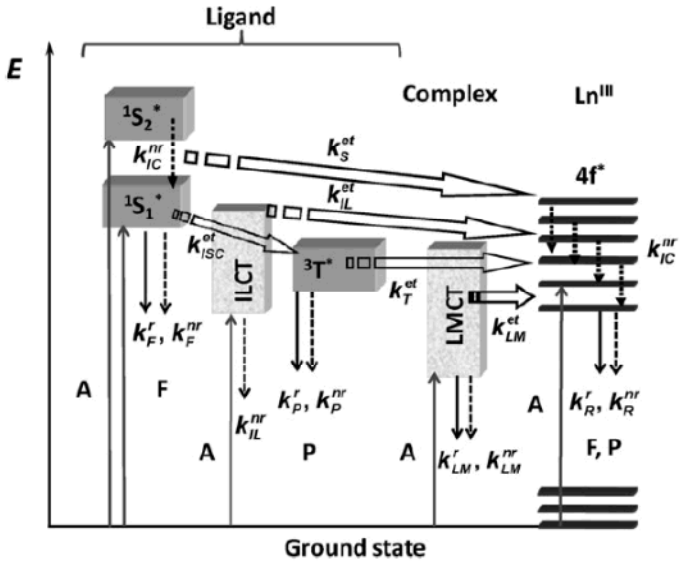

Figure 6. Schematic representation of energy absorption, migration, emission (plain arrows), and dissipation (dotted arrows) processes in a lanthanide complex. $^1S^*$ or S = singlet state, $^3T^*$ or T = triplet state, A = absorption, F = fluorescence, P = phosphorescence, *k* = rate constant, *r* = radiative, *nr* = non-radiative, IC = internal conversion, ISC = intersystem crossing, ILCT (indices IL) = intra-ligand charge transfer, LMCT (indices LM) = ligand-to-metal charge transfer. Back transfer processes are not drawn for the sake of clarity. [44] Reproduced by permission of The Royal Society of Chemistry (RSC).

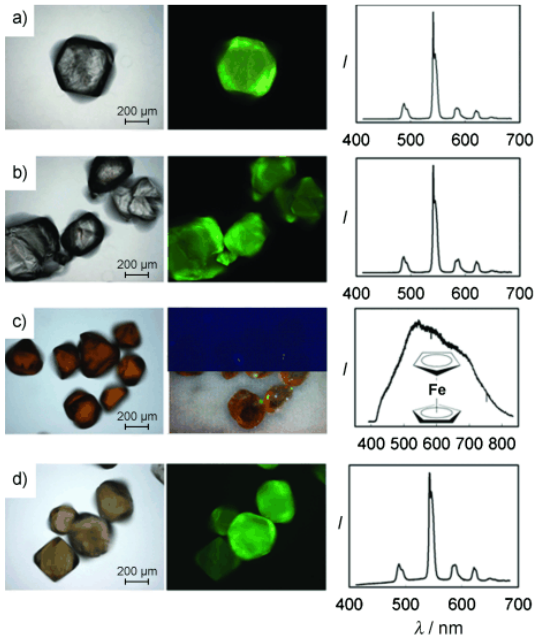

Figure 7. Transmission (left) and fluorescence (middle) microscope images and luminescence spectra (right) for a) a single MOF, b) multiple MOFs, c) ferrocene included MOFs, and d) regenerated initial MOFs after removal of ferrocene via evacuation at 50 °C for 1 day. In the fluorescence image of c), half of the background color was subtracted to show the crystals. [71] Copyright Wiley-VCH Verlag GmbH & Co. KGaA. Reproduced with permission.

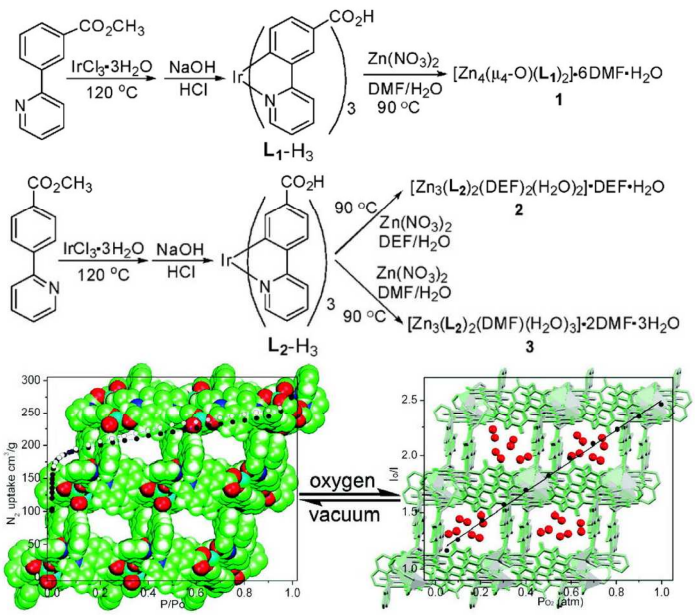

Figure 8. (Top) Three structures were synthesized from Ir tris(2-phenylpyridine)-based ligands. **1** was found to be porous, showing rapid and reversible luminescence quenching by oxygen, as shown schematically (bottom). Reprinted with permission from [99]. Copyright 2010 American Chemical Society.

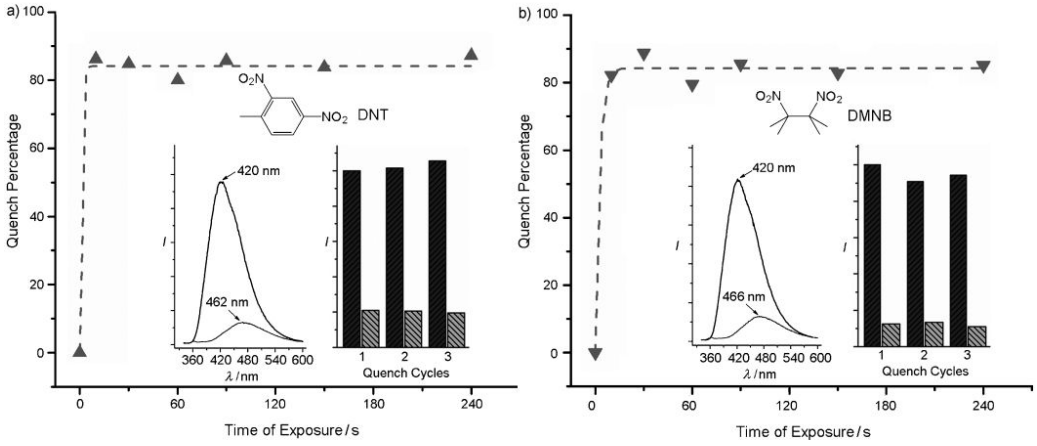

Figure 9. Time-dependant fluorescence quenching of MOFs by DNT and DMNB. The red-shifted fluorescence can be seen in the inset, along with three quench/fluorescence regeneration cycles. [100] Copyright Wiley-VCH Verlag GmbH & Co. KGaA. Reproduced with permission.

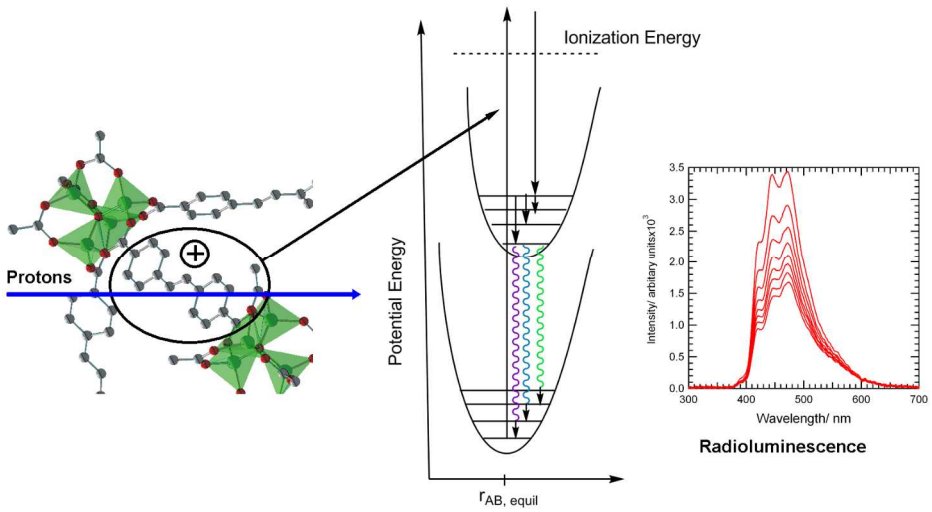

Figure 10. Schematic of the fast neutron detection process. Left: Interaction of high energy recoil protons with a rigid stilbene unit (a portion of the cubic 3D stilbene MOF structure is shown with stilbene dicarboxylate linkages between tetrahedral Zn_4O units), resulting in excitation, which decays (center) through radiationless pathways (solid arrows) to the lowest-lying excited state of the stilbene groups, followed by radiative decay and emission of photons (wavy arrows). The emission profile is shown on the right, revealing diminishing intensity upon repeated doses of high intensity radition.

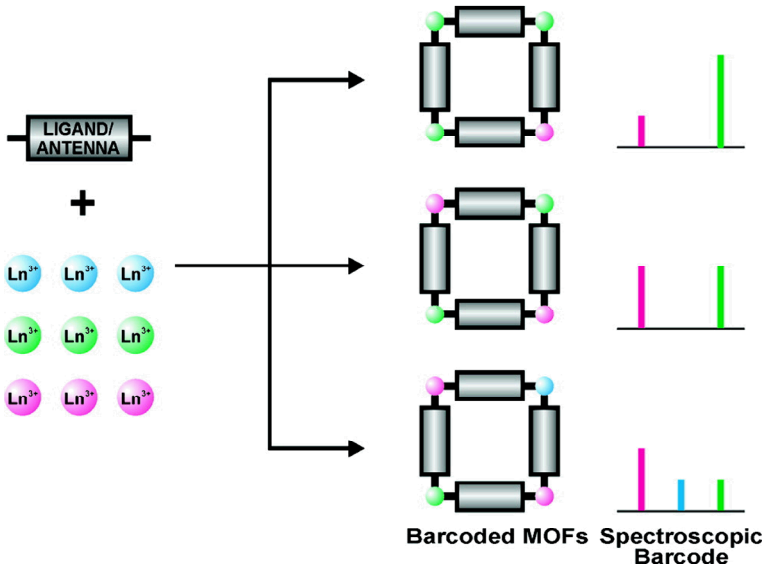

Figure 11. Schematic of the development of luminescent barcode materials by controlling the relative amounts of three differing emissive lanthanide ions in the MOF structures. Reprinted with permission from [116]. Copyright 2009 American Chemical Society.